Available online at www.sciencedirect.com

SCIENCE DIRECT®

Global and Planetary Change 46 (2005) 101–124

GLOBAL AND PLANETARY CHANGE

www.elsevier.com/locate/gloplacha

Internal carbon and nutrient cycling in Lake Baikal: sedimentation, upwelling, and early diagenesis

Beat Müller*, Martin Maerki, Martin Schmid, Elena G. Vologina[1], Bernhard Wehrli, Alfred Wüest, Michael Sturm[2]

Swiss Federal Institute of Environ. Sci. Technol. (EAWAG), Federal Institute of Technology (ETH), Limnological Research Center, CH-6047 Kastanienbaum, Switzerland

Federal Institute of Technology (ETH), Limnological Research Center, CH-6047 Kastanienbaum, Switzerland

Received 1 November 2004; accepted 1 November 2004

Abstract

The internal cycles of carbon, silica, nitrogen, and phosphorus in the South and North Basins of Lake Baikal were quantified in the frame of a multidisciplinary collaboration. Fluxes of particulate organic matter from the epilimnion to the deep water were quantified with integrating sediment traps deployed at 200- to 250-m water depth and compared with fluxes measured in near-bottom traps to reveal mineralization in the water column. Sedimentation rates were determined with dated sediment cores to calculate mass accumulation rates of elements in the sediment. Advective and turbulent transport of dissolved nutrients in the water column was based on a set of monitoring data, which included temperature and current data, as well as hydrochemical data of the water column. Diffusive fluxes from the sediment to the overlying water column were determined by applying different porewater sampling techniques. The combination of these data resulted in consistent internal budgets for carbon, nitrogen, and phosphorus in Lake Baikal: the new production in the South Basin was 1730 mmol C m^{-2} $year^{-1}$ and the mass accumulation rate in the sediment 220 mmol C m^{-2} $year^{-1}$, whereas in the more secluded North Basin, new production was only 1220 mmol C m^{-2} $year^{-1}$ and mass accumulation rate 125 mmol C m^{-2} $year^{-1}$. Fluxes of particle-bound nitrogen, phosphorus, and biogenic silica were by about 30% smaller in the North Basin than in the South Basin. Export fluxes of nitrogen from the surface zone to the deep water were 150 mmol N and 100 mmol N m^{-2} $year^{-1}$. Denitrification rates in the sediment were estimated from mass-loss calculation to 38 and 53 mmol N m^{-2} $year^{-1}$ for the South and North Basin, respectively, corresponding to 25% and 52% of the total nitrogen input to the hypolimnion. Nitrogen (19 and 13 mmol m^{-2} $year^{-1}$) was finally buried in the sediments of the South and North Basins; 10.1 and 3.5 mmol P m^{-2} $year^{-1}$, and 1830 and 1400 mmol Si m^{-2} $year^{-1}$ were transferred to the deep water in the South and North Basin where 28% and 70% P, and 64% and 54% Si were retained in the sediments. A diatom bloom occurred during our sampling period of 2

* Corresponding author. Tel.: +41 41 349 21 49; fax: +41 41 3492 168.
E-mail address: beat.mueller@eawag.ch (B. Müller).
[1] RAS-SB, Institute of Earth Crust, Irkutsk, Russia.
[2] EAWAG, CH-8600 Dübendorf, Switzerland.

0921-8181/$ - see front matter
doi:10.1016/j.gloplacha.2004.11.008

years, which usually occurs only every 3 to 5 years. Accordingly, Si flux data from sediment traps were increased by an estimated 50% compared with the long-term average illustrating the necessity of several years of field measurements to compensate for the natural dynamics of Lake Baikal.

Keywords: Lake Baikal; sediment; nutrient cycle; sediment traps; porewater; turbulence; advection

1. Introduction

Lake Baikal is one of the world's great ancient lakes and home to a unique variety of more than 1000 endemic species ranging from diatoms, sponges to salmonid fish, and the Baikal freshwater seal (Kozhova and Izmest'eva, 1998). Most of the catchment of 540,000 km^2 with its ~350 rivers is only scarcely populated and thus contributes little to anthropogenic contamination of the lake. Its water column is permanently oxic with a very constant chemical composition (Falkner et al., 1991), and primary productivity is limited by the availability of phosphate. The Selenga River contributes 50% of the water and 75% of the particle load to the lake carrying the anthropogenic load of the growing cities of Ulan-Ude and Ulan-Bator. Moreover, large pulp mill and galvanizing industries of the town of Baikalsk at its southern shore and enhanced tourist activities are a serious threat to the fragile ecosystem of the lake (Kozhova and Izmest'eva, 1998; Shimaraev et al., 1994). The risk of such potential changes for the lake's unique ecosystems can only be assessed if the internal fluxes of biomass and nutrients are known in greater detail.

The age of Lake Baikal is estimated to be between 30 to 40 million years, the surface area is 31,500 km^2, and, at 1637 m, it is the deepest lake on earth. It lies in the tectonic rift zone between Europe and Asia and has never been permanently ice-covered during the last ice age (Back et al., 1999). The lake freezes annually between January and May in the South Basin and between December and June in the North Basin. Its sedimentary deposits of more than 7 km bear a treasure of information on continental paleoclimates. In order to link this long-term record with the environmental conditions that the lake was exposed to, it is essential to establish a consistent lake-internal mass balance of the present sedimentation regime and element cycling, which involve the principal biogenic components, such as organic carbon, nitrogen, phosphorus, and silica.

In recent years, different studies have been published on the water budget, distribution of major elements, characterization of suspended particulate matter, and sediments of Lake Baikal. Partly published in Russian, these papers were reviewed by Callender and Granina (1997b) and Granina (1997). The integrating budget approach in their studies is based on an in- and output model, which has been used to estimate accumulation rates of a variety of chemical parameters. However, no study has been done which investigated the cycling of major nutrients determining export from the epilimnion to deeper water layers, gross and net sedimentation (total settling material reaching the lake bottom, and material finally buried in the sediment after early diagenesis), mineralization, and turbulent and advective transport of solutes in the water column of Lake Baikal. Early diagenetic processes and the formation of iron/manganese crusts in the upper layers of the sediment were described and discussed by Deike et al. (1997) and Müller et al. (2002). The new production (export of organic carbon from the epilimnion) was estimated to be 27 g C m^{-2} $year^{-1}$ by Weiss et al. (1991). Several physical studies focussed on large-scale advective transport and small-scale turbulent mixing processes, concluding that the average renewal time of the bottom water masses, i.e., the time since their last contact with the lake surface, was only in the range of 7 to 19 years (Weiss et al., 1991; Hohmann et al., 1997, 1998; Peeters et al., 1997; Kodenev et al., 1998). This efficient deep-water renewal is unusual considering the large depth of the lake (1637 m) and the overall hydrological water residence time of about 330 years. Investigations on mass accumulation rates and mineralization processes of organic material during settling have not been published for Lake Baikal until now. A better understanding of the processes governing this lake ecosystem can be

achieved by detailed investigation of the cycle of phytoplankton nutrients and the settling and mineralization of autochthonous biogenic material. This paper is primarily based on results of the EC-funded transdisciplinary project CONTINENT and some additional sites studied in former projects. The objectives of this study were to quantify: (I) the fluxes of dissolved major algal nutrients and of particle bound elements (organic carbon, nitrogen, phosphorus, and biogenic silica) between the compartments surface water, deep water, and surface sediments; (II) the mineralization of particulate organic carbon during settling through the deep water and after deposition at the lake bottom; and (III) the chemical dissolution of biogenic silica in the hypolimnion and in the surface sediments in bulk budgets for the related elements.

Individual flux rate estimates are based on: (a) sediment trap data from 200- to 250-m depth and the lake bottom; (b) bulk sediment composition of radiometric-dated sediment cores; (c) estimates on advective and turbulent water exchange between surface and deep water, based on chemical profiles of the water column, water current, and temperature data; (d) sediment porewater profiles of nitrate, ammonium, phosphate, and silica; and (e) the estimation of aerobic mineralization rates of organic carbon in the surface sediments via O_2 flux rate calculations based on measured O_2 porewater concentration gradients at the sediment–water interface.

2. Study site and methods

2.1. Moorings and CTD profiles

Three mooring strings with sediment traps were deployed between 2001 and 2002 (Fig. 1). At the mooring in the North Basin, temperatures were recorded every 10 min with eight Richard Brancker TR-1000 temperature recorders at 16-, 174-, 227-, 389-, 550-, 740-, 795-, and 868-m water depth. Eight integrating sediment traps were exposed at 225-, 335-, 445-, 555-, 720-, 775-, 885-, and 903-m depth. In the central South Basin mooring, 5 VEMCO minilogs recorded temperatures every 60 min at 16-, 41-, 75-, 100-, and 195-m depth, and 11 R. Brancker TR-1000/1050 every 10 min at 303-, 350-, 397-, 445-, 540-, 825-, 1015-, 1210-, 1305-, 1352-, and 1396-m depth. At both moorings, amplitude and direction of currents were measured every 30 min with an Aanderaa current meter 1.5 m above the lake floor. Fifteen integrating sediment traps were placed in 40-, 100-, 255-, 350-, 445-, 540-, 635-, 730-, 825-, 922-, 1015-, 1113-, 1210-, 1305-, and 1396-m depth. At the Neutrino Site mooring, again in the South Basin, four VEMCO and three TR 1050 loggers recorded temperatures at 19-, 43-, 81-, 184-m depth, and 284-, 382-, and 1363-m depth, respectively. Fourteen integrating cylindrical traps were exposed at 100-, 200-, 300-, 400-, 510-, 600-, 700-, 800-, 900-, 1000-, 1100-, 1200-, 1300-, and 1350-m depth. Deployment and recovery of the moorings were carried out with RV Vereshagin of the Limnological Institute, Irkutsk, and from the ice (Neutrino site). Profiles of conductivity, temperature, and depth (CTD) were measured with a SeaBird SBE-25 probe at 31 stations throughout the lake during the research cruise in July 2002 and at 37 stations in July 2003.

2.2. Sediment sampling and analysis

In the summers of 2001, 2002, and 2003, a number of short cores were withdrawn with a modified gravity corer (Kelts et al., 1986). The corer allowed sampling of the uppermost 140 cm without destruction of the sediment–water interface. Selected master cores from Continent Ridge, Posolskoe High, Vydrino Shoulder, and the central South Basin (Fig. 1; positions given in Appendix A) were extruded in sampling intervals of 0.5 cm until 5-cm depth, and then every 1 cm for the rest of the core. A fraction of each sample was transferred to a plastic bag and transported to EAWAG (Switzerland) for the determination of the water content (loss of weight at 60 °C). Samples were centrifuged to separate porewater on board ship. Pellets remaining after centrifugation were packed in polycarbonate boxes and transported to EAWAG, where they were freeze-dried, ground in an agate mortar, and acid-digested with 4 ml of HNO_3 (conc., suprapure) and 1 ml of H_2O_2 in a microwave oven. P_{tot} was determined as o-PO_4 after digestion with potassium peroxodisulfate. C_{org} and N_{tot} were analyzed with a CNS-Analyzer after expelling inorganic carbon with H_3PO_4. Biogenic silica was analyzed by ICP-OES (Spectro Analytical Instruments) after leach-

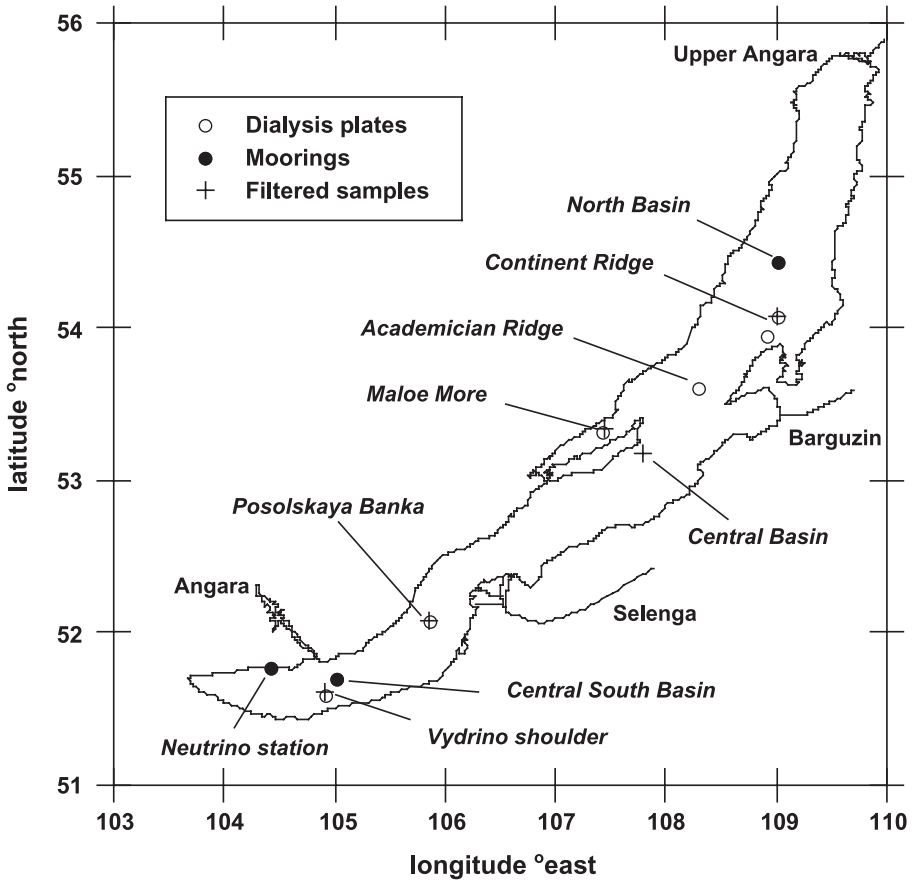

Fig. 1. Map of Lake Baikal indicating mooring sites for the Continent project and sampling locations of the master sediment cores sampled for the CONTINENT project and porewater profiles obtained with diffusion plates and filtration.

ing of 30 mg of sample aliquots with 1 N NaOH solution at 90 °C for 3 h (Mortlock and Froehlich, 1989). Activities of ^{137}Cs and ^{210}Pb in the sediments were determined by gamma-spectrometry in Ge–Li borehole detectors. As ^{137}Cs is mobile in sediments of Lake Baikal, ^{210}Pb was used for core dating and estimation of sedimentation rates (Hakanson and Jansson, 1983; Appleby, 2000). The mean standard error was between 15% and 20% depending on the ^{210}Pb activity. Sedimentation rates (mm year^{-1}) were determined using ^{210}Pb isotope measurements in the top 5 cm.

Mass accumulation rates (MAR) for C_{org}, N_{tot}, Si_{bio}, and P_{tot} were averaged for the samples of 0.5- to 5-cm depth and calculated correcting the volume sedimentation rate (SR) [mm year^{-1}] with porosity (ϕ) and sediment density (ρ_{sed}) [g cm^{-3}] (data see Appendix A):

$$\mathrm{MAR} = \mathrm{SR}\rho_{\mathrm{sed}}10^{3}(1-\phi) \quad (1)$$

Sediment density (ρ_{sed}) was averaged for the samples of 2- to 8-cm depth and calculated from C_{org} measurements (in percent) with the relationship:

$$\rho_{\mathrm{sed}} = -0.0523C_{\mathrm{org}} + 2.65. \quad (2)$$

Porosity (ϕ) was calculated from water content (WC) of the sediment and the sediment density (ρ_{sed}):

$$\phi = \frac{\mathrm{WC}\rho_{\mathrm{water}}}{\mathrm{WC}\rho_{\mathrm{water}} + (1-\mathrm{WC})\rho_{\mathrm{sed}}} \quad (3)$$

where ρ_{water} is the density of water (=1 g cm^{-3}), WC the water content in [%/100]. Mean porosity of the top 5 cm was used to calculate mass accumulation rates.

2.3. Porewater sampling and analysis

Two dialysis samplers (Hesslein, 1976; Urban et al., 1997) with 1-cm vertical resolution and 50-cm length were exposed to collect porewater profiles of the uppermost 50 cm sediment in 1996, 2001, and 2002 (Fig. 1). Each dialysis sampler was mounted on a tripod and lowered to the sediment on a rope secured on surface buoys during exposition. Oxygen contamination was prevented with protecting plates that were released before the retrieval of the samplers. Exposition time was 6 to 10 days, depending on the ship schedule. Cellulose acetate membranes of 0.2-μm pore size were used. Porewaters were sampled from six sites, i.e., Maloe More, Academician Ridge, Posolskoe High, Vydrino Shoulder, Continent Ridge, and the North Basin (positions and porewater concentrations are given in Appendix B). Furthermore, in 2003, porewater was obtained by filtration of extruded slices of sediment with a filter paper (Schleicher and Schuell LS14, Germany) and a small vacuum pump (KNF Neuberger, Switzerland) to avoid stress on the sediment particles, and subsequent filtration through 0.45 μm cellulose acetate membranes. Apart from Academician Ridge, the same positions were chosen for porewater filtration as for the dialysis samplers and thus data can be compared (Appendix C)). Porewater samples were additionally recovered with a whole-core squeezer (Bender et al., 1987; Jahnke, 1988), and by centrifugation of 0.5 to 1 cm sections of the sediments and subsequent filtration (cellulose acetate filters, 0.45 μm) during expeditions in 2001 and 2002.

Porewater samples were conserved with 0.2% chloroform and analyzed at EAWAG, Switzerland, for NO_3^-, NH_4^+, SiO_2, and o-PO_4 using standard photometric methods (DEW, 1996). In 2002, NH_4^+ in porewater was measured on board of the research vessel with the indophenol method (DEW, 1996) and a portable photometer (Merck Spectroquant). In March and July 2001, porewater measurements of O_2, NO_3^-, and NH_4^+ were performed with ion-selective electrodes on retrieved sediment cores from the South Basin, Vydrino, and Posolskoe High on the ice and in the hydrological institute on shore at Listvijanka to give vertical concentration profiles with high spatial resolution. Measurements are described in detail by Maerki et al. (submitted for publication). Diffusive fluxes across the sediment–water interface were calculated from the chemical gradients of their porewater concentration profiles assuming steady-state conditions and using Fick's first law of diffusion (Berner, 1980):

$$J_i = -\frac{D_0^i}{F} * \frac{dc_i}{dz} \quad (4)$$

J_i is the flux of solute i across the sediment–water interface, D_o^i the diffusion coefficient of the species i in pore water at 5 °C (Li and Gregory, 1974), F is a factor correcting for the sediment porosity and tortuosity (F=1.2; Maerki et al., 2004), dc_i/dz is the concentration gradient at the sediment surface.

2.4. Calculation of turbulent and advective transport of dissolved elements

The efficient deep-water renewal in Lake Baikal, and with it the transport of dissolved substances between the surface and the deep waters, is due to strong turbulent mixing and the episodic advective transport of surface water to the deep water. These two processes are shortly described below and represented in Fig. 2. Additional information is given in Appendix D.

2.4.1. Turbulent transport

Vertical diffusivity (K_z) in Lake Baikal has been studied with temperature microstructure and dissipation measurements (Ravens et al., 2000), using temperature profiles (Shimaraev and Granin, 1991; Ravens et al., 2000), chlorofluorocarbons, helium, tritium, or dissolved oxygen as tracers (Killworth et al., 1996; Peeters et al., 2000), as well as by balancing biogeochemical water constituents and turbulent energy (Wüest et al., 2000). The various methods applied lead to K_z estimates of 1 to 90 cm^2 s^{-1}, values that are unusually high compared to other lakes. Using all available information, vertical diffusivity K_z at 400-m depth was estimated to 12.5 cm^2 s^{-1} with an error of ~25% (Wüest et al., 2000) for the South Basin and 8 cm^2 s^{-1} for the North Basin.

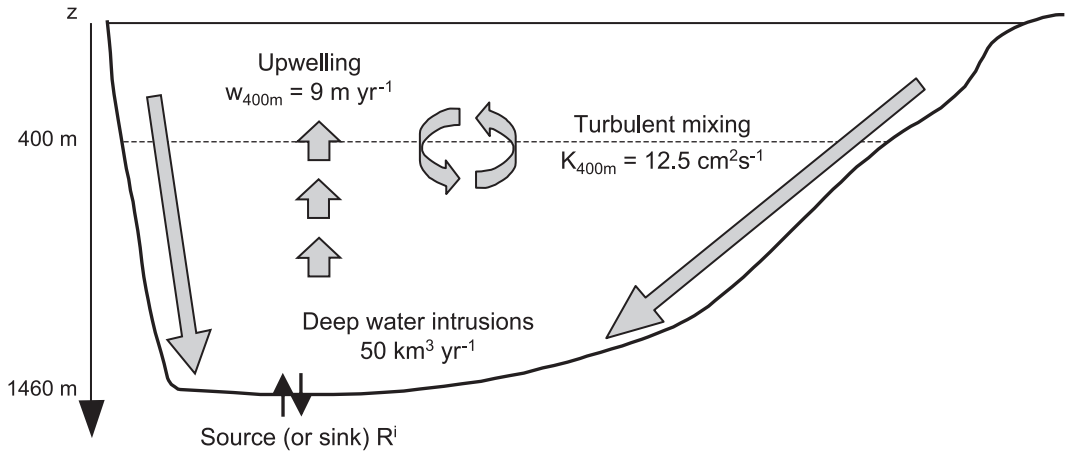

Fig. 2. Overview of the processes considered in the calculation of the element fluxes for the South Basin. Due to continuity, the deep intrusions are compensated by a large-scale upwelling of the internal layers (≈9 m year^{-1}).

2.4.2. Advective transport

The top 250–300 m of the surface waters of Lake Baikal are convectively mixed twice every year, usually in December/January and in June (Shimaraev et al., 1994). During these periods, intrusions of cold surface water to the deepest layers of the lake have been regularly observed (Wüest et al., 2005). Annual volumes of these intrusions were roughly estimated to 30 to 70 km^3 for both the South and the North Basins. In the following, we assume a deep-water formation rate of 50 km^3 year^{-1} for both basins. The deep-water formation must be balanced by upwelling to close the water balance. The respective average upwelling velocities at 400-m depth are 9 and 5 m year^{-1} for the South and the North Basins.

This knowledge about the turbulent and advective transport was used to derive the simple budget presented in Eq. (5) for the transport of dissolved substances, based on an approach developed by Munk (1966) for the ocean. This approach allows estimation of the fluxes of O_2, N, P, and Si between surface and deep waters of Lake Baikal, based on the steady-state assumption that the temporal change of the concentrations of these substances can be neglected. Except for silica (see discussion in the Results section), this assumption has been confirmed by concentration measurements (Domysheva, 2001). The deep water is defined here as the water mass below 400-m depth, which is a safe distance from the depth of 250–300 m that is reached by seasonal convective mixing and the sill level. The budget of a dissolved substance i in the deep water can then be calculated with:

$$-K_{400\mathrm{m}}\frac{\partial c^i}{\partial z}+w_{400\mathrm{m}}\left(c^i_{\mathrm{SL}}-c^i_{400\mathrm{m}}\right)+R^i = H_{400\mathrm{m}}\frac{\partial c^i}{\partial t}=0 \quad (5)$$

where $K_{400\mathrm{m}}$ is the vertical diffusivity at 400-m depth, c^i is the concentration of the species i, c^i_{SL} is its concentration in the intruding water masses (which is assumed to be the same as in the surface waters), c^i_{400} is the concentration at 400-m depth, $w_{400\mathrm{m}}$ is the upwelling velocity that compensates the volume flow of the deep-water intrusions, R^i is the source (R^i<0) or sink (R^i>0) of i below 400-m depth including the fluxes from and to the sediment, $H_{400\mathrm{m}}$ ($=V_{400}/A_{400}$) is the average depth below 400 m (V_{400} and A_{400} are volume below and area at 400-m depth, respectively), and the z-axis is pointing downwards. The first term of Eq. (5) is the turbulent transport from the deep water to the surface water, while the second term describes the replacement of deep water with surface water by advective transport. These two terms are negative, when the flux is directed from the deep water to the surface, and their sum must be balanced by the source or sink term R^i. In order to obtain basin-scale mass balances, the specific fluxes obtained from Eq. (5) have to be multiplied by the basin area at 400-

m depth. A_{400} is 5500 km^2 in the South Basin and 10,000 km^2 in the North Basin.

2.5. Calculation of element cycles for C, N, P, and Si

There are two approaches for establishing budgets of carbon, nitrogen, phosphorus, and silica in a deep lake. The first is the application of a one-box model to the lake basin, which results in the assumption of a balance between the external input of an element i, F^i_{in} (from rivers and from the atmosphere), the outflux, F^i_{out}, and the final annual mass accumulation of an element in the sediment after early diagenesis, defined here as net sedimentation, S^i_{net}, which is quantified from dated sediment cores:

$$z_b \frac{dc^i_b}{dt} = F^i_{\text{in}} - F^i_{\text{out}} - S^i_{\text{net}} \quad (6)$$

c^i_b is the concentration of an element i in the lake basin, b. Fluxes are normalized to the area of the basins with units of mol m^{-2} year^{-1}. Therefore, the annual change of concentration in the lake basin, dc^i_b/dt, is multiplied with the average depth of the basin, z_b. We will assume steady-state conditions $dc^i_b/dt=0$, if not stated otherwise.

In the second case, we consider a hypolimnion mass balance in order to establish lake internal element budgets. Observations from sediment traps and sediment cores allow a budget of the particulate matter fluxes, and a two box-model is used as sketched in Fig. 3, with one box comprising the deep water and the second box including the diagenetically active zone of the sediment. S^i_{exp} denotes the particulate flux of i exported from the productive zone into the deep-water and is measured by sediment traps at 200 to 250 m, well below the thermocline. Gross sedimentation S^i_{gr} is the flux of particulate elements from the deep water to the lake bottom and quantified by bottom trap data. On their way to the lake bottom through the deep-water, settling particles are affected by chemical dissolution and microbially mediated degradation. The net mass release to the hypolimnion from sedimenting particles, R^i_{dh}, is then given by:

$$R^i_{\text{dh}} = S^i_{\text{exp}} - S^i_{\text{gr}}. \quad (7)$$

The two other processes contributing to the fluxes of dissolved components in the hypolimnion are related (i) to the sum of advective and turbulent transport, F^i_{at} across the thermocline (see 'section calculation of turbulent and advective transport') and (ii) to the diffusive flux across the sediment–water interface, F^i_{dif} (see chapter 'porewater sampling and analysis'). Both fluxes are positive along the z-axis, which points to fluxes towards the sediment. This

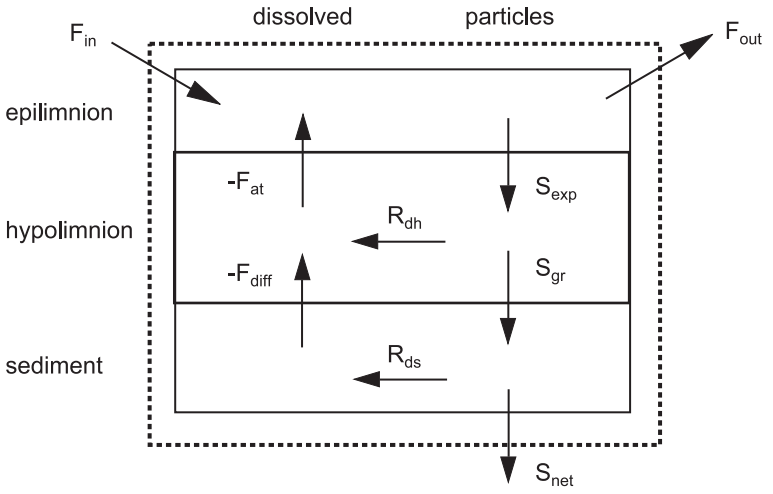

Fig. 3. Fluxes of elements in biogeochemical cycles for Lake Baikal. The figure highlights a two-box model comprising deep-water and the zone of the sediment–water interface.

allows the formulation of a mass balance for dissolved components i in the hypolimnion of a lake basin:

$$z_h \frac{dc_h^i}{dt} = F_{at}^i - F_{dif}^i + R_{dh}^i \quad (8)$$

where z_h denotes the average depth of the hypolimnion. Steady-state conditions are assumed in the hypolimnion with $dc_h^i/dt=0$. The release of C, N, P, and Si from settling particles to the deep water, and R_{dh}^i, can alternatively be calculated from physical transport of solutes in the deep-water, fluxes of dissolved components from or to the sediment and sediment burial. $^*R_{dh}^i$, in Eq. (9) is independent from sediment trap data if the mineralization of organic carbon is calculated from O_2 concentration profiles:

$$^*R_{dh}^i = F_{dif}^i - F_{at}^i - S_{net}^i. \quad (9)$$

Thus, it is an independent way of quantifying the degradation of organic carbon, which is indicated by the star (*). We assume total oxic mineralization and Redfield composition for the settling organic material in the water column (O_2/C=138:106).

Some of the biogenic material collected in sediment traps is lost during exposition due to dissolution or mineralization. For the sediment traps at 200–250 m depth, this was corrected with the factor f_1, which assumes that S_{exp}^i should be equal to the sum of the net sedimentation and physical transport out of the deep water:

$$f_i = \frac{S_{net}^i + F_{at}^i}{S_{exp}^i} \quad (10)$$

Gross sedimentation can be related to the sum of net sedimentation plus diffusion from the porewater to the lake bottom water, leading to a correction factor f_2:

$$f_2 = \frac{S_{net}^i + F_{dif}^i}{S_{gr}^i} \quad (11)$$

The probable loss of silica from the sediment traps is due to dissolution of diatom frustules rather than microbial degradation, although certain diatom species are more susceptible to dissolution processes than others (e.g., Ryves et al., 2003). Thus, the different processes may cause rather different loss of silica than for C, N, and P, and we did not correct for it. Since silica is the major part of the settling material, mass accumulation was also left uncorrected.

3. Results

3.1. Fluxes of N, Si, P, and O_2 across the sediment–water interface

Fluxes of nutrients and oxygen were calculated from chemical concentration gradients in sediments using data either measured with ion-selective electrodes in sediment cores, or collected with diffusion plates and filtration. As these samples were collected with a minimum of force exerted on the sediment particles, we consider the obtained results to be more reliable than those based on squeezed and centrifuged samples. Concentrations obtained by the latter techniques tended to be higher and, thus, resulted in systematically higher fluxes. This may be an artefact caused by the strong physical perturbation of the sediment. Therefore, data from samples gathered by diffusion plates and filtration are presented separately and in more detail, while all other data are given as mean values with standard deviations in Table 1.

3.1.1. Nitrate

NO_3^- concentrations were very low in Lake Baikal sediments (around 10 μmol l^{-1}), and hence, reproducibility of analytical determinations was hampered. In some porewater profiles, peaks of NO_3^- were detected in a zone of 1–2 cm below the sediment–water interface. However, these peaks were difficult to resolve spatially and to sample for chemical analysis. Measurements with ion-selective electrodes (Maerki et al., submitted for publication) confirmed the occasional occurrence of concentration maxima for NO_3^- as well as for NH_4^+ in the top few millimeters of the sediment. Fluxes derived from diffusion plate experiments from the North and South Basins ranged from 7 to 31 mmol m^{-2} $year^{-1}$ to give a mean of 22 mmol N m^{-2} $year^{-1}$, which is identical to the fluxes estimated from microelectrode porewater concentration profiles (data not shown). Porewater results from sediment filtration samples (marked method "F" in Table 1) range from 45 to 130 mmol N m^{-2} $year^{-1}$, where all fluxes were directed from the bottom water to the sediment porewater. Porewater concentration peaks cause very steep gradients, which lead to very high fluxes in both directions, into the bottom water as well as

Table 1
Fluxes determined from porewater concentration profiles, F^{i}_{dif}

Site	Method	Year	Depth	NO_3^-	NH_4^+	SiO_2	o-PO_4
			[m]	[mmol m^{-2} $year^{-1}$]			
Maloe More	D	1996	125	20	−20	−296	−19.0
	F	2003		130	−270	−223	−20.1
Academ. Ridge	D	1996	280	no	−2.9	−347	−0.5
Posolskoe High	D	2001	160	7.3	−23	−237	−3.1
	F	2003		45	−300	−241	−1.4
Vydrino Shoulder	D	2001	674	31	−30	−110	−2.4
	F	2003		55	−320	−288	−0.8
Continent Ridge	D	2002	360	no	−4.7	−183	−3.5
	F	2003		63	−300	−139	−2.6
North Basin	D	2002	792	31	−12	−128	−3.7
Central Basin	F	2003	1636	47	−340	−318	−8.4
North Basin, averages (*n*)	S/C			150±120 (9)	−30±34 (10)	−1030±460 (12)	−3.5±2.2 (13)
South Basin, averages (*n*)	S/C			17±2.7 (2)	−82±42 (5)	−940±530 (5)	−6.0±0.5 (2)

"D" and "F" indicate that porewater was collected with diffusion plates or filtration of sliced sediment cores, respectively. "S" and "C" indicate porewater sampled with squeezer and centrifuge. Numbers of samples for calculated averages are given in parenthesis. Negative values signify fluxes from the sediment porewater to the bottom water, positive values vice versa. "no" indicates that no clear concentration gradient was expressed. Concentration data are given in Appendix B and C. Location of sites, see Fig. 1 [methods: diffusion plate (D); filter (F); squeeze/centrifuge (S/C)].

deeper into the sediment. However, the narrow concentration maxima may be a seasonal effect and may occur only during short time periods. Thus, fluxes estimated from such concentration patterns probably do not reflect steady-state situations and may not be representative for average annual N-fluxes. Flux calculations based on squeezed or centrifuged samples from 17 locations in the North and South Basin resulted in average fluxes of 150±120 and 17±2.7 mmol m^{-2} $year^{-1}$, respectively, directed from the water to the sediment (marked "S/C" in Table 1).

3.1.2. Ammonium

NH_4^+ concentration maxima in narrow zones of 1–2 cm were detected with all sampling facilities and ion-selective electrodes. The same arguments as for NO_3^- apply here as well. Fluxes may not be representative for the annual average but rather reflect a summer situation after the settling of spring diatom blooms. Fluxes determined from samples collected with diffusion plates varied between −2.9 and −30 mmol N m^{-2} $year^{-1}$. Results showed that mineralization was higher around the Selenga Delta and the South Basin, which are influenced by the load of organic matter of this river, than in the North Basin and at Academician Ridge, which is characterized by smaller sedimentation rates and thus smaller quantities of settled organic carbon. NH_4^+ analysis of porewater samples recovered by squeezing or centrifugation yielded much higher flux rates with −270 to −340 mmol N m^{-2} $year^{-1}$, not sensitive for differences between the North and South Basins.

3.1.3. Silica

The diffusive flux of dissolved Si from the surface sediment into the overlaying water column is driven by the concentration gradient of Si across the sediment–water interface. The concentration gradient is maintained through continuous dissolution of siliceous biogenic matter in the surface sediment, which mainly originates from settled diatoms. Fluxes from diffusion plates and porewater filtration ranged from −110 to −347 mmol m^{-2} $year^{-1}$ with lowest values in the North Basin and Continent Ridge. Silica fluxes determined for the South and North Basins on the basis of centrifugation or squeezers averaged −1030±460 and −940±530 mmol m^{-2} $year^{-1}$, respectively

3.1.4. Phosphate

For the period between 1994 and 2003, 38 flux rate estimates for phosphate were calculated for various sites of the lake basin (Fig. 4). Values were quite

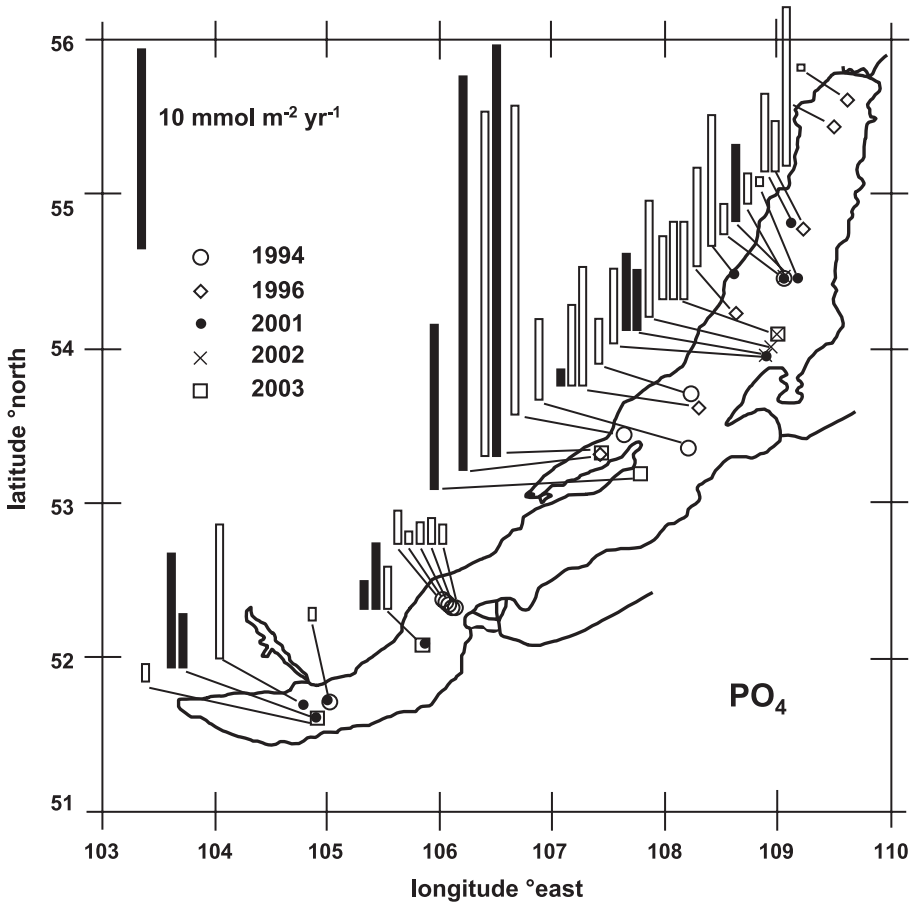

Fig. 4. Overview of sediment fluxes determined for o-PO_4 during the expeditions of 1994, 1996, 2001, 2002, and 2003. Filled bars represent data from diffusion plates ("D") and filtration ("F"), empty bars indicate data from centrifuged ("C") and squeezed ("S") sediment samples.

evenly distributed over the whole lake (-4.0 ± 3.7 mmol m^{-2} $year^{-1}$) except for significantly higher fluxes in the bay of Maloe More with its sandy sediments (-19 to -20 mmol m^{-2} $year^{-1}$). The very small fluxes in the Selenga Delta area (-0.5 to -3.1 mmol m^{-2} $year^{-1}$) and at two locations in the South Basin (-0.8 to -2.4 mmol m^{-2} $year^{-1}$) were striking, but two independent techniques (diffusion plates and filtration) showed similar concentration profiles. They probably indicate the role of Fe-oxyhydroxide particles in the sediment as an efficient sink for phosphorus. The Selenga Delta is an accumulation zone for terrigenous particles, and sediments from Academician Ridge and the North Basin show discrete Fe–Mn precipitates (Granina et al., 2004).

3.1.5. Oxygen

Average fluxes of O_2 from the bottom water into the sediment were 1200 ± 400 mmol m^{-2} $year^{-1}$ estimated from multiple microelectrode porewater profiles at five locations in the South Basin. For the North Basin, an O_2 flux of 400 mmol m^{-2} $year^{-1}$ was extracted from microelectrode profiles published by Martin et al. (1998). Mineralization of organic carbon was calculated from O_2 fluxes applying the Redfield ratio. Values representative for porewater fluxes of N, P, and Si in the South Basin were considered averages from measurements at Vydrino shoulder and Posolskoe High. Values for the North Basin were averaged from data of Continent Ridge and North Basin in Table 2.

Table 2
Fluxes of carbon and nutrients across the sediment–water interface, advective and turbulent transport, and estimated river imports and exports

Param.	Loc.	Diffusive flux from/to sediment	Turbulent+ advective transport	Riverine import	Riverine export
		F^i_{dif}	F^i_{at}	F^i_{in}	F^i_{out}
		[mmol m^{-2} $year^{-1}$]			
O_2	SB	1200[a] (±35%)	2300 (±30%)		
	NB	400[b] (±35%)	1300 (±30%)		
C	SB	1030[c] (±35%)	1730[c] (±30%)	800[d]	200[d]
	NB	340[c] (±35%)	1030[c] (±30%)		
N	SB	19 (NO_3^-) (±88%) −26 (NH_4^+) (±19%)	−93 (NO_3^-) (±70%)	49[e]	22[e]
	NB	31 (NO_3^-) (−) −12 (NH_4^+) (−)	−34 (NO_3^-) (±70%)		
P	SB	−2.0 (±53%)	−5 (±60%)	2[e] 7[f]	1[e] 1[f]
	NB	−3.2 (±18%)	−3 (±60%)		
SiO_2	SB	−220 (±35%)	−630 (±40%)	300[e,f,g]	74[e]
	NB	−150 (±19%)	−460 (±40%)		

Values for fluxes across the sediment surface are selected averages from Table 1 for the South Basin (SB; mean of Vydrino and Posolskoe High) and North Basin (NB; Continent Ridge and North Basin). Negative values indicate upward fluxes, from the sediment to the bottom water, or from the deep water to the surface and vice versa. In parenthesis are the estimated mean standard errors in percent.

[a] Maerki et al. (submitted for publication).
[b] Martin et al. (1998, Fig 2a; 820-m depth).
[c] Calculated from the O_2 flux using the Redfield ratio O_2/C=1.38:1.06.
[d] Granina (1997).
[e] Tarasova and Mescheryakova (1992).
[f] Callender and Granina (1997b).
[g] Granina et al. (2000).

3.2. Advective and turbulent transport of dissolved substances in the water column

Eq. (5) was checked using the vertical concentrations measured in July 1988 by Weiss et al. (1991) and on several occasions in the years 1993–1999 by Domysheva (2001). All available concentration profiles were averaged, and gradients were calculated for the depth range between 300 and 800 m, where constant gradients within the measurement error were observed. For the further discussion, we used the calculations based on the more recent data by Domysheva (2001). The resulting total turbulent and advective fluxes are presented in Table 2 and described in detail below. For all elements, the turbulent fluxes are much more important than the advective fluxes as they contribute 70–95% to the total fluxes.

3.2.1. Oxygen

The calculated turbulent fluxes of O_2, based on the concentrations measured by Domysheva (2001), at a depth of 400 m are 1900 (South Basin) and 1100 (North Basin) mmol O_2 m^{-2} $year^{-1}$, the total fluxes including advection 2300 (South Basin) and 1300 (North Basin) mmol O_2 m^{-2} $year^{-1}$. These results are comparable to data reported by Kipfer et al. (2000) who calculated a total flux of 530 mmol O_2 m^{-2} $year^{-1}$ to the sediment and reported a consumption of 2.8 mmol O_2 m^{-3} within the deep water, which would sum up to a flux of ~1600 mmol O_2 m^{-2} $year^{-1}$ for the South Basin and ~900 mmol O_2 m^{-2} $year^{-1}$ for the North Basin.

3.2.2. Nitrogen

The NO_3^- gradients measured by Domysheva (2001) are less steep than those measured by Weiss et al. (1991). The first yields turbulent NO_3^- fluxes of −67 mmol m^{-2} $year^{-1}$ in the South Basin and −23 mmol m^{-2} $year^{-1}$ in the North Basin, respectively, and total fluxes including advection of −93 mmol m^{-2} $year^{-1}$ in the South Basin and −34 mmol m^{-2} $year^{-1}$ in the North Basin. Weiss et al. (1991) measured total fluxes of −144 mmol m^{-2} $year^{-1}$ (South Basin) and −63 mmol m^{-2} $year^{-1}$ (North Basin), respectively. Further calculations are based on the recent Domysheva (2001) data, and the discrepancies with earlier studies are discussed later. Transport of dissolved N as NH_4^+ can be neglected since permanently oxic conditions in the water column and the surface sediments allow fast nitrification.

3.2.3. Phosphate

Phosphate gradients reported by Domysheva (2001) result in a total flux of −5 (South Basin) and −3 mmol m^{-2} $year^{-1}$ (North Basin), those reported by Weiss et al. (1991) result in total fluxes of −9 (South Basin) and −6 mmol m^{-2} $year^{-1}$(North Basin), respectively.

3.2.4. Silica

The average concentration gradients measured by Domysheva (2001) were 15 μmol Si m^{-4} (South

Basin) and 17 (North Basin) μmol Si m^{-4}, yielding a turbulent flux of −580 (South Basin) and −440 mmol m^{-2} $year^{-1}$ (North Basin). Compared to the turbulent flux, the advective transport of −51 (South Basin) and −22 mmol m^{-2} $year^{-1}$ (North Basin) is small. The total fluxes are −630 (South Basin) and −460 mmol m^{-2} $year^{-1}$ (North Basin). If the system was in a steady state, these fluxes should be balanced by the release of Si from the sediment. However, Shimaraev and Domysheva (2002) observed an annual decrease in Si concentrations of approximately 1000 (South Basin) and 500 mmol m^{-2} (North Basin) below 400-m depth during the years 1995–2001. This observed decrease in Si concentrations is larger than the calculated physical transport. This means that the steady-state assumption is not valid for this element and that our model is not sufficient to explain the observations; an additional Si sink from the hypolimnion would be needed to balance the observed decrease in Si concentrations.

3.3. Net sedimentation

Four master cores were selected, representative for the Continent Ridge in the North Basin with low sedimentation rates, the small underwater hill Posolskoe High in the vicinity of the Selenga delta, Vydrino Shoulder in the South Basin, and the deepest point in the South Basin (Fig. 1). Estimates of net sedimentation rates in different parts of Lake Baikal critically evaluated by Granina et al. (2004) compare well with our measured values listed in Table 3. With ^{210}Pb dating of the top 5 cm of each core, we obtained 1.5 mm $year^{-1}$ on Posolskoe High, triggered due to its vicinity to the Selenga Delta. Distinctly lower values of 0.57 mm $year^{-1}$ were measured on the Continent Ridge. Sedimentation rates at Vydrino Shoulder were within a range of 0.52 mm $year^{-1}$ and 1.0 mm $year^{-1}$. A value of 0.47 mm $year^{-1}$ was estimated for the central South Basin. Applying these sedimentation rates to the analytical data obtained from the respective cores revealed mass accumulation rates for C_{org}, N, P, and Si_{bio} listed in Table 3. For total particulate matter as well as C_{org}, N, and P highest deposition rates were observed at Posolskoe High. Sedimentation at this underwater mound was dominated by the particulate input of the Selenga, which was the cause for these high settling rates. Therefore, data from Posolskoe High were excluded from the calculation of the mean net sedimentation of the South Basin. Mass accumulation rates of C_{org}, N, and Si_{bio} were comparable for the remaining two sites in the South Basin and were clearly higher than in the North Basin.

Table 3
Net sedimentation, S^i_{net}, of total particulate matter, C_{org}, N_{tot}, Si_{bio}, and P_{tot} calculated from the four "CONTINENT project Master Cores" (Fig. 1)

Coring site	Sed. rate [mm $year^{-1}$]	Total mass [g m^{-2} $year^{-1}$]	C_{org}	N_{tot}	Si_{bio}	P_{tot}
			[mmol m^{-2} $year^{-1}$]			
Continent Ridge (NB)	0.57	68	125	14	780	2.6
Posolskoe High (SB)	1.49	266	567	56	1090	8.5
Vydrino Shoulder (SB)	0.75	143	251	18	1300	3.5
Central South Basin (SB)	0.47	89	193	19	1080	2.2
Averaged C/N/Si/P			68	6.4	253	1

The P-standardized ratio of C/N/Si/P was calculated from averages of all elements. Sediment data used are given in Appendix A.

3.4. Export production and gross sedimentation

For the first time, flux rate estimates based on sediment trap measurements are available for Lake Baikal, and results from the North Basin can be compared with results from two sites of the South Basin, the central South Basin mooring, and the Neutrino mooring 3.5 km off shore in the South Basin (Fig. 1). Table 4 lists fluxes of total particulate matter as well as C_{org}, N_{tot}, Si_{bio}, and P_{tot} that quantify gross sedimentation. However, these numbers must be corrected for mineralization and dissolution in the traps during exposition as described above. We exemplify this procedure for carbon in the South Basin and calculate f_1 according to Eq. (10). Using 1730 mmol C m^{-2} $year^{-1}$ for the physical transport F^i_{at} and mean values for South Basin net sedimentation S^C_{net} (220 mmol C m^{-2} $year^{-1}$) and the export of organic carbon from the epilimnion S^C_{exp} (960 mmol C m^{-2} $year^{-1}$; Table 4), we calculate for f_1=2.03. For gross sedimentation (Eq. (11)), we used the mean value of S^C_{gr} 675 mmol C m^{-2} $year^{-1}$ (Table 4) and 920 mmol C m^{-2} $year^{-1}$ for F^C_{dif} (Table 2), which results in f_2=1.69. We used the average of f=1.8 to correct all sediment trap measurements for organic carbon. Correction factors for N and P were deviating

Table 4
Particle fluxes and gross sedimentation of nutrients in the central South Basin, Neutrino Site, and North Basin

Mooring site	Date	Depth	Total mass	C_{org}	N_{tot}	Si_{bio}	P_{tot}
		[m]	[g m^{-2} $year^{-1}$]	[mmol m^{-2} $year^{-1}$]			
Central South Basin	Mar 01–Jul 02	255	138	992	93	3120	5.7
		1305	117	664	67	2140	5.0
Neutrino Site	Mar 01–Mar 02	200	126	929	73	2290	9.5
		1300	136	685	64	2420	4.7
North Basin	Jul 01–Jul 02	225	63	678	55	1400	2.6
		885	94	375	30	2320	2.7
Averaged C/N/Si/P				143	12.7	454	1

Values are not yet corrected for mineralization in the trap during exposition. Samples at 200 to 255 m represent the export from the epilimnion to the deep water, while the traps in the deep water were used to quantify gross sedimentation. The P-standardized ratio of C/N/Si/P was calculated from averages of all elements. All measurements used are given in Appendix E.

from those determined for organic carbon due to the inaccuracy in the calculation of fluxes from concentration gradients that were close to the analytical detection limit. Due to similar C/N ratios observed in sediment trap material (11.3; Table 4) and in the sediment (10.8; Table 3), we used the same factor for N as for organic carbon. However, C/P ratios were 143 in sediment traps and only 69 in the sediment. This comparison indicates that P is much stronger retained in the sediment than C and N. Since the P-fraction doubles from the trap material to the sediment, and C- and N-fractions decompose twice as fast as the P-fraction, we estimated that only 25% of the total P-fraction had decomposed in the cylinder traps. Hence, a correction factor f=1.33 was estimated by this method. Corrected values of the sediment trap data averaged for South and North Basins are given in Table 5. Average values from the sediment traps at central South Basin and Neutrino site are used in the nutrient balance of the South Basin. Export of organic carbon from the epilimnion to the deep water of the lake is the new production. Export fluxes, S^i_{exp}, from the epilimnion to the deep water were obtained at 200–250 m, and gross sedimentation, S^i_{gr}, from the second lowest traps. Mineralization of organic carbon, dissolution of biogenic silica, and release of P and N in the hypolimnion, respectively, was calculated by the difference in particulate weights between the upper trap and the next to last bottom trap.

Table 5
Particle fluxes corrected for mineralization and dissolution during exposition in the traps

Site	Variable	Total mass	C_{org}	N_{tot}	P_{tot}	Si
		[g m^{-2} $year^{-1}$]	[mmol m^{-2} $year^{-1}$]			
South Basin	S^i_{exp}	132	1730	150	10.1	2700
	S^i_{gr}	126	1220	120	6.5	2280
North Basin	S^i_{exp}	63	1220	100	3.5	1400
	S^i_{gr}	94	675	55	3.6	(2320)

Values for the South Basin were averaged from the central South Basin mooring and Neutrino Site (Table 4). Samples at 200 to 255 m represent the export from the epilimnion to the deep water (S^i_{exp}), while the traps in the deep water were used to quantify gross sedimentation (S^i_{gr}).

Particle fluxes in Lake Baikal are preferentially governed by settling of particles from the epilimnion into the deep hypolimnion of the lake. No significant difference in the composition of the trap material between upper and lower traps was observed. It consists mainly of diatoms, organic debris, and lithogenic particles. Increased values of particle fluxes in traps above the sediment are due to the existence of a benthic boundary layer (BBL) with enhanced particle concentration and increased turbulence at the sediment–water interface (Ryves et al., 2003; Wüest et al., 2005). Annual fluxes showed significant differences between the North and South Basins in total material, C_{org}, N_{tot}, and P_{tot} with fluxes 30% (C and N) and 65% (P) lower in the North Basin compared to the South Basin. Little difference was observed in the Si_{bio} flux. Data from the two South Basin moorings compared well except for strikingly high values of silica in the upper traps in the central South Basin and P in upper traps at the Neutrino Site.

4. Discussion

4.1. Settling particulate matter

The net mass accumulation rate of settled material from bottom sediment traps was 127 g m^{-2} $year^{-1}$ (average of the bottom traps central South Basin and the Neutrino Site; Table 4). This agreed well with the mean mass accumulation rate of particulate matter for the South Basin of 89–143 g m^{-2} $year^{-1}$ determined from the sediment cores from Vydrino and the central South Basin stations (Table 3). Thus, dissolution of bulk material from the sediment was not apparent from weight difference. Chemical analysis revealed that the majority of the settling material was biogenic silica, which has a very low dissolution rate compared to fresh organic material. The trap material consisted of 50.2% biogenic silica and only 6.4% organic carbon. Our accumulation rates of particulate matter corresponded well with data from various other authors. From measurements of suspended sediments by Tarasova and Mescheryakova (1992), Granina (1997) calculated a sedimentation rate of 3680 kt $year^{-1}$ (117 g m^{-2} $year^{-1}$), which compared well with the 3560 kt $year^{-1}$ (113 g m^{-2} $year^{-1}$) estimated by Callender and Granina (1997a).

4.2. Organic carbon

The balance of particulate organic carbon in the South Basin is shown in Fig. 5a. It combines the organic carbon flux estimates based on sediment trap data with estimates for the mineralization rate of organic carbon in the deep water and the surface sediment, which are based on O_2 measurements in the water column and at the sediment–water interface. Sediment trap data that were used to quantify the export of organic carbon from the epilimnic zone to the deep water and thus the new production yield S^{C}_{exp}=1730 mmol C m^{-2} $year^{-1}$ and a gross sedimentation in the bottom trap of S^{C}_{gr}=1220 mmol C m^{-2} $year^{-1}$. The value for the new production compares relatively well with earlier measurements by Weiss et al. (1991), who estimated 2250 mmol C m^{-2} $year^{-1}$. Our estimate for the net accumulation of organic carbon, S^{C}_{net}, of 220 mmol m^{-2} $year^{-1}$ (mean value from the two sites in the South Basin; Table 3) is lower than a previous estimate of 330 mmol m^{-2} $year^{-1}$ by Votintsev and Popovskaya quoted in Granina (1997). Weiss et al. (1991) estimated a sequestration of only 83 mmol m^{-2} $year^{-1}$ of organic carbon in the sediments, which in comparison seems rather low. The mineralization rate of organic matter in the water column as determined from the weight

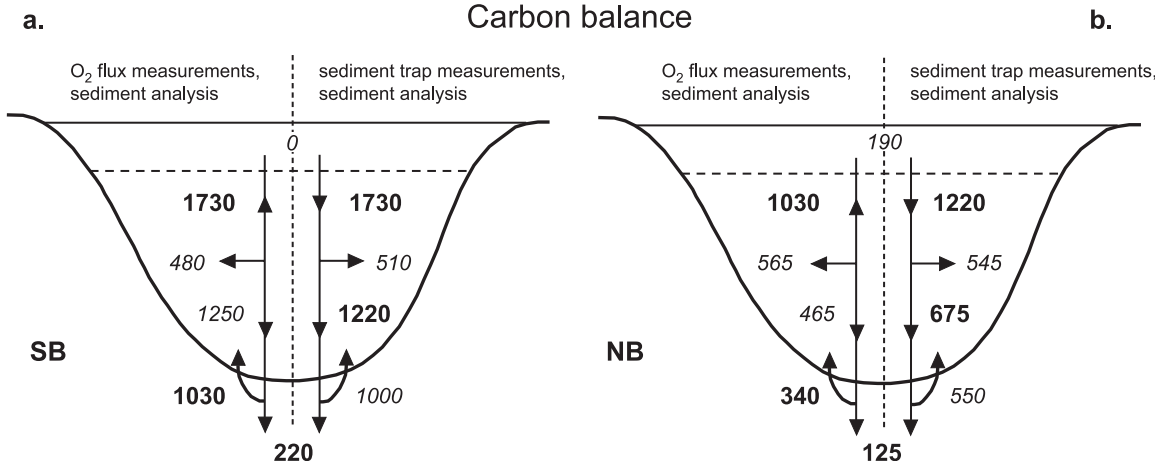

Fig. 5. Budget for carbon in the (a) South Basin and (b) North Basin of Lake Baikal. Fluxes are in mmol m^{-2} $year^{-1}$. Bold numbers are based on analytical measurements; numbers in italic indicate the difference between fluxes. Numbers on the left-hand side represent mineralization of organic carbon estimated from advective and turbulent O_2 flux measurements in the water column and across the sediment–water interface. The right-hand side depicts results from sediment trap measurements (export from epilimnion to the deep water, gross sedimentation). The bottom number in the middle is the mass accumulation rate of organic carbon as determined from sediment analysis.

difference between the sediment traps was R^{C}_{dh}=510 mmol m^{-2} $year^{-1}$.

The total of the advective and turbulent O_2 flux from the surface water into the deep water (F^{O2}_{at}) is 2300 mmol O_2 m^{-2} $year^{-1}$. Assuming steady-state conditions, this value corresponds to a total mineralization rate (F^{C}_{at}) of 1730 mmol C m^{-2} $year^{-1}$, if Redfield composition is assumed for the settling particles. The flux of particulate organic carbon exported from the surface water to the hypolimnion is given by the sum of the above estimated mineralization rate in the deep water (F^{C}_{at}) and the net accumulation rate of organic carbon in the sediment (S^{C}_{net}) of 220 mmol C m^{-2} $year^{-1}$ to be S^{C}_{exp}=1950 mmol C m^{-2} $year^{-1}$. Fluxes of O_2 into the sediment at five locations in the South Basin were calculated from porewater gradients measured with microelectrodes yielding a mean value of F^{O2}_{dif}=1200±400 mmol O_2 m^{-2} $year^{-1}$ (Maerki et al., submitted for publication). Assuming complete oxidation of settled organic matter and composition of settling particles given in Table 4, this diffusive flux corresponds to a mineralization rate of organic carbon in the sediment (R^{C}_{ds}; Fig. 3) of 1030 mmol C m^{-2} $year^{-1}$. Since 1730 mmol C m^{-2} $year^{-1}$ has been mineralized totally according to the O_2 transport to the deep water, 1030 mmol C m^{-2} $year^{-1}$ was consumed by aerobic mineralization in the sediment and 220 mmol C m^{-2} $year^{-1}$ buried, the difference of $*R^{C}_{dh}$=480 mmol C m^{-2} $year^{-1}$ must have been degraded in the water column. This value is close to the corresponding estimate based on the weight difference of the sediments trapped of 510 mmol C m^{-2} $year^{-1}$. In the water column of 1100-m magnitude (distance between the two sediment traps), the average of 500 mmol C m^{-2} $year^{-1}$ corresponds to a volume rate of 0.45 mmol C m^{-3} $year^{-1}$.

The release of carbon from the sediment, which is calculated by the difference between gross sedimentation and net sedimentation, of 1000 mmol m^{-2} $year^{-1}$ corresponds closely to F^{C}_{dif} of 1030 mmol m^{-2} $year^{-1}$ determined from O_2 sediment porewater microelectrode measurements. The close agreement of the results obtained by measurements of two independent parameters, particulate organic carbon and dissolved O_2, suggests a good accuracy for our flux estimates.

In the North Basin mass accumulation rates, weight of settling particles, sediment porewater fluxes as well as transport processes in the water column of carbon were systematically 25–50% smaller than in the South Basin. The net mass accumulation rates in the bottom sediment traps and in the sediment were only 94 and 68 g m^{-2} $year^{-1}$, respectively. The North and South Basin of Lake Baikal are rather different with respect to input loads, temperature of the productive zone, duration of ice cover etc. This is well reflected in the nutrient flux data. A summarized mass balance is represented in Fig. 5b. New production of organic carbon transported into the deep waters of the North Basin, S^{C}_{exp}, was 1220 mmol C m^{-2} $year^{-1}$ (or 14.6 g C m^{-2} $year^{-1}$) and thus 30% lower than in the South Basin. Gross sedimentation (675 mmol C m^{-2} $year^{-1}$) and net sedimentation (125 mmol C m^{-2} $year^{-1}$) were both 44% smaller in the North than in the South Basin. The mineralization rate of organic carbon in the diagenetically active zone of the sediment as calculated by the difference of gross and net sedimentation was 550 mmol m^{-2} $year^{-1}$.

O_2 profiles across the sediment–water interface could not be measured in the North Basin. However, O_2 consumption of North Basin sediment was extracted from a microelectrode concentration profile recorded by Martin et al. (1998, Fig. 2a; 820-m depth) to calculate a flux of 400 mmol O_2 m^{-2} $year^{-1}$, which converts to a mineralization, F^{C}_{dif}, of 340 mmol C m^{-2} $year^{-1}$. This is three times less than what we found for the South Basin and agrees with the trend to significantly lower mineralization rates in the north. Mineralization of organic carbon in the water column, F^{C}_{at}, estimated from physical transport and O_2 concentration profiles, amounts to 1030 mmol C m^{-2} $year^{-1}$. Total organic carbon exported from the epilimnion estimated as the sum of F^{C}_{at} and S^{C}_{net} was 1155 mmol C m^{-2} $year^{-1}$, which compared well with the result from sediment trap measurements (1220 mmol C m^{-2} $year^{-1}$). The rate of organic matter mineralized in the hypolimnion calculated from the difference between F^{C}_{dif} and (F^{C}_{at}+S^{C}_{net}) of 565 mmol C m^{-2} $year^{-1}$ corresponded well with the rate determined from the weight loss between upper and lower sediment traps of 545 mmol C m^{-2} $year^{-1}$.

4.3. Nitrogen

The export of particulate organic-bound N to the deep water of the South Basin, S^{N}_{exp}, was 150 mmol

m^{-2} $year^{-1}$ and gross sedimentation, S^N_{gr}, was 120 mmol m^{-2} $year^{-1}$ (Fig. 6a). Only 19 mmol N m^{-2} $year^{-1}$ was buried in the sediment. Estimates of net sedimentation in the Russian literature range from 23 to 41 mmol m^{-2} $year^{-1}$ (Granina, 1997). The net flux of NO_3^- from the deep water to the surface water by turbulent diffusion and advection was F^N_{at}=−93 mmol m^{-2} $year^{-1}$. This returning flux of NO_3^- is only about 60% of the particulate organic nitrogen exported with the settling biomass. Due to permanently oxic water column and the top few centimeters of surface sediments, denitrification in Lake Baikal occurs only in the sediments. An indirect estimate for denitrification by mass loss can be obtained from $S_{exp}-S_{net}+F_{at}$=38 mmol N m^{-2} $year^{-1}$ assuming steady-state conditions for fluxes and reservoir concentrations. This corresponds to 25% of the N from organic matter input to the hypolimnion. This denitrification rate is in the order of the average marine denitrification rate (285 Tg N $year^{-1}$ or about 57 mmol m^{-2} $year^{-1}$) by Middelburg et al. (1996). Final burial in the sediments is about 12% of the export production. The recovered porewater profiles of NO_3^- and NH_4^+ showed a substantial spatial and seasonal variability (Table 1, see discussion in the Results section). NO_3^- concentrations were around 10 μmol l^{-1} and close to the analytical detection limit. In some porewaters, distinct peaks were detected within a zone of 1–2 cm and, thus, difficult to spatially resolve for sampling. Accordingly, fluxes from these maxima were then directed to the water column as well as to the sediment. The same patterns were observed for NH_4^+ as well. Such porewater maxima induce very steep concentration gradients and thus very high fluxes. They may, however, not reflect a sustainable annual average. The peaks may be a seasonal pattern and originate from the settling of spring diatom blooms that are quickly mineralized. The processes of mineralization of organic-bound N to NH_4^+, its subsequent nitrification in aerobic sediment and the denitrification of NO_3^- at the oxic–anoxic interface to elemental N_2 are processes that are not distinguishable with the present dataset. Thus, the contribution of sediment porewater concentrations of dissolved N-species cannot be quantified.

N-fluxes in the North Basin were about one-third smaller than in the south. From the sediment traps, we estimated fluxes S^N_{exp}= 100 and S^N_{gr}=55 mmol m^{-2} $year^{-1}$ for the traps at 225 and 885 m, and a net sedimentation, S^N_{net}, of 13 mmol m^{-2} $year^{-1}$ (Fig. 6b). Physical transport from the deep water to the epilimnion was −34 mmol m^{-2} $year^{-1}$. Thirteen percent of the exported particle-bound N was buried in the sediment, 53% may have been denitrified as calculated with the abovementioned formula, and the remaining 34% transported to the epilimnion by advection and turbulence. The large fraction of nitrogen undergoing denitrification in the North Basin with its lower productivity should not be stressed. The relatively large errors accumulate when the fluxes

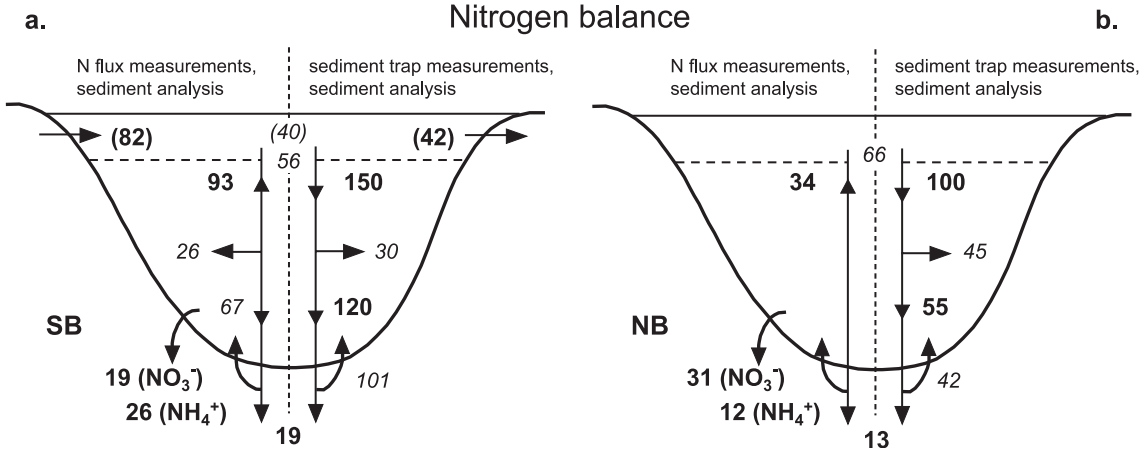

Fig. 6. Budget for nitrogen in the (a) South Basin and (b) North Basin of Lake Baikal. Fluxes are in mmol m^{-2} $year^{-1}$. Bold numbers are based on analytical measurements; numbers in italic indicate the difference between fluxes. Numbers in parenthesis depict import and export estimates from Granina (1997).

obtained with three different methods are used for the calculation of denitrification by mass loss.

The internal mass balance including our estimates for denitrification rates can now be compared with published external mass balances for the South Basin. For the quantification of the nitrogen budget, Tarasova and Mescheryakova (1992) suggested a load of 21.7 kt year^{-1} and an output through the Angara River of 9.7 kt year^{-1} translating into a nitrogen elimination of only 27 mmol m^{-2} year^{-1}. Other authors arrived at higher external nitrogen loads of up to 36.1 kt year^{-1} for the input and 18.3 kt year^{-1} for the output (Granina, 1997) with a corresponding nitrogen elimination rate of 40 mmol m^{-2} year^{-1}. This latter value is closer, but still 30% lower than our estimate of nitrogen elimination (denitrification plus burial) of 57 mmol m^{-2} year^{-1}.

4.4. Phosphorus

A critical evaluation of available data by Granina (1997) for P suggests an average input by tributaries and atmosphere of 6.4 kt year^{-1} (F^{P}_{in}=6.6 mmol m^{-2} year^{-1}), output of 1.2 kt year^{-1} (F^{P}_{out}=1.2 mmol m^{-2} year^{-1}) and thus a sediment accumulation of 5.2 kt year^{-1} (5.4 mmol m^{-2} year^{-1}). Our measurements showed a net P mass accumulation, S^{P}_{net}, in the South Basin of only 2.2–3.5 mmol m^{-2} year^{-1}, however, up to 8.4 mmol m^{-2} year^{-1} was measured at Posolskoe High with its high particle settling rate. We suppose that the difference between the load given by Granina (1997) and the calculations from our own measurements originates from the particulate P buried in the river deltas. Moreover, we may have underestimated P net sedimentation since we ignored local formations of Fe/Mn crusts in the sediment, which show high P concentrations bound by sorption and/or coprecipitation (Müller et al., 2002). In addition, retention of P in the sediment was much more heterogeneous than for C, Si, or N, and release rates varied from very low (Academician Ridge) to very high values (Maloe More). High P dissolution in the bay of Maloe More coincides with the local occurrence of the diatom species Stephanodiscus meyerii (Fig. 3 in Mackay et al., 2003), a genus which is typical for meso- to eutrophic lakes. Flux data are presented in Fig. 7. Particulate export from the surface waters, S^{P}_{exp}, is 10.1 mmol P m^{-2} year^{-1} while 6.5 mmol m^{-2} year^{-1} calculates for gross sedimentation, S^{P}_{gr}. Twenty-eight percent of the particulate P transported into the deep water is buried in the sediment, which is twice as much as was determined for N. The prominent feature supporting small dissolved porewater P concentrations is the deep penetration depth of O_2 into the sediment and the availability of sorbing Fe-oxyhydroxide surfaces.

Sedimentation and turbulent transport of P in the North Basin was again significantly smaller than fluxes in the South Basin. P contents in the sediment traps of all depths were about the same, while 45% of both, C and N, disappeared between surface and

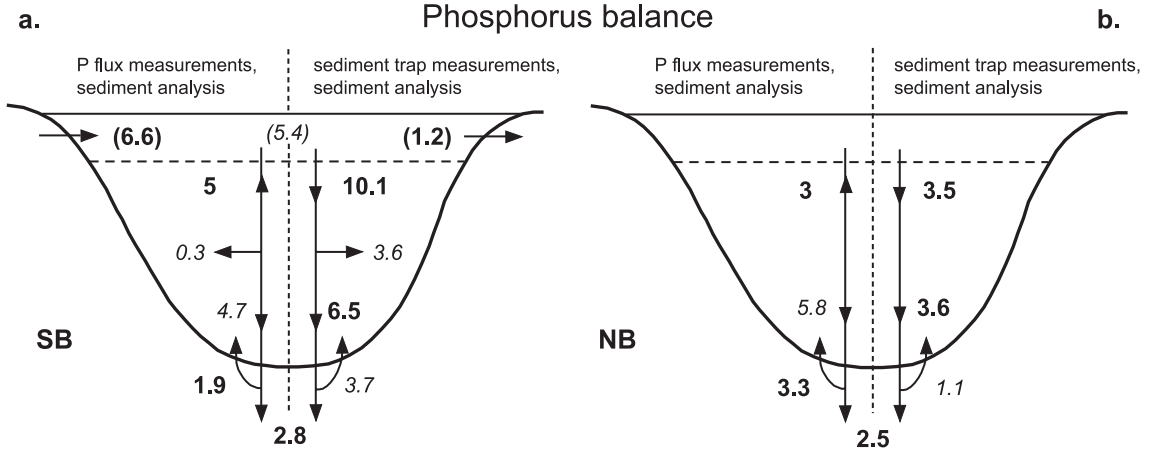

Fig. 7. Budget for phosphorus in the (a) South Basin and (b) North Basin of Lake Baikal. Fluxes are in mmol m^{-2} year^{-1}. Bold numbers are based on analytical measurements; numbers in italic indicate the difference between fluxes. Numbers in parenthesis depict import and export estimates from Granina (1997).

bottom traps. Net sedimentation was about the same in both basins. Therefore, the sediments in the North Basin are trapping P more effectively than in the South Basin. This again is most probably linked to the deeper oxygen penetration depths and the higher concentration of iron/manganese crusts in the sediments of the North Basin (Müller et al., 2002; Granina et al., 2004).

4.5. Biogenic silica

The degradation pathway of organic material does not apply for silica, which undergoes mainly abiotic dissolution, and, thus, silica may not be affected noticeably in the sediment traps during storage time. The biological cycles in Lake Baikal are dominated by the growth and mineralization of diatoms, and the sediment consists mainly of diatom frustules and silty clay (Vologina et al., 2003). Thus, silica is the key constituent in the quantification of formation and dissolution of these sediment markers and climate proxies. We determined an average of S^{Si}_{exp}=2700 mmol m^{-2} $year^{-1}$ of Si_{bio} transported into the deep waters of the South Basin, and a gross sedimentation, S^{Si}_{gr}, of 2280 mmol m^{-2} $year^{-1}$ (Table 5). Net sedimentation was S^{Si}_{net}=1170 mmol m^{-2} $year^{-1}$ (Fig. 8a). Callender and Granina (1997b) suggested a riverine input and export of dissolved silica of F^{Si}_{in}=312 mmol m^{-2} $year^{-1}$ and F^{Si}_{out}=74 mmol m^{-2} $year^{-1}$, respectively. C_{org}, N, and P in the core from Posolskoe High near the Selenga Delta reached two or three times the values from other cores, except for Si_{bio}, which was similar to the contents of the other two cores from the South Basin. Dissolution of silica from the sediment, R^{Si}_{ds}, was on average 240 mmol m^{-2} $year^{-1}$ and could be determined quite reliably due to clear concentration gradients in the porewaters. Concentrations of Si were substantially increased when centrifugation or squeezing was applied to gain porewaters. Fluxes of dissolved Si calculated from porewater concentration profiles from five different sites obtained with centrifugation and squeezing of the sediment resulted in 940±530 mmol m^{-2} $year^{-1}$ (marked "S/C in Table 1). Modeling advective and turbulent fluxes in the water column from the concentration gradient resulted in a flux of Si from the bottom water to the epilimnion of F^{Si}_{at}=630 mmol m^{-2} $year^{-1}$. Callender and Granina (1997b) suggested a riverine input and export of dissolved silica of F^{Si}_{in}=312 mmol m^{-2} $year^{-1}$ and F^{Si}_{out}=74 mmol m^{-2} $year^{-1}$, respectively.

The data on Si-fluxes in Lake Baikal show a considerable unbalance with respect to this element. There are two major points which need further discussion. First, our model cannot explain the observation of Shimaraev and Domysheva (2002) that concentrations of dissolved Si in the hypolimnion of the South basin were decreasing by 1000 mmol m^{-2} $year^{-1}$ during 1995–2001. This amount of Si in addition to that released by the sediment and by

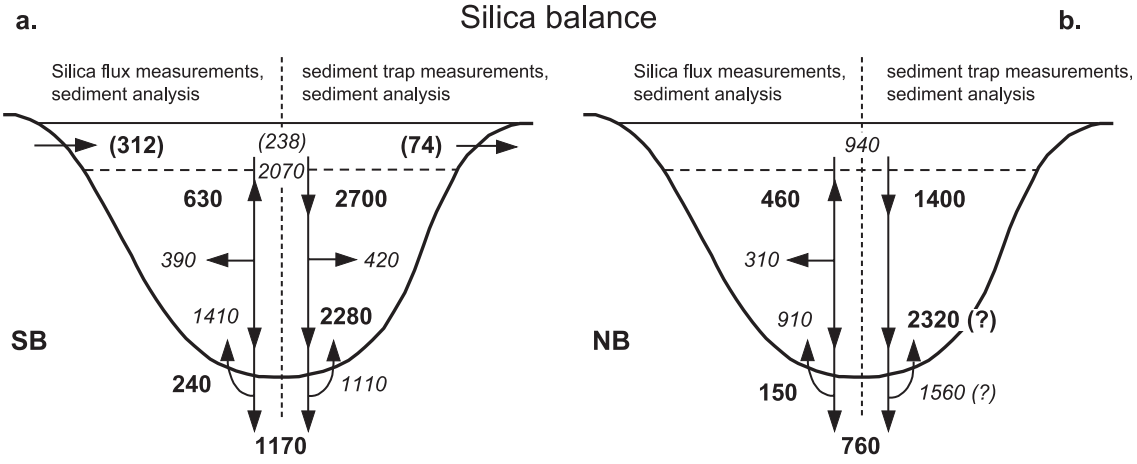

Fig. 8. Budget for silica in the (a) South Basin and (b) North Basin of Lake Baikal. Fluxes are in mmol m^{-2} $year^{-1}$. Bold numbers are based on analytical measurements; numbers in italic indicate the difference between fluxes. Numbers in parenthesis depict import and export estimates from Callender and Granina (1997b).

settling particles could not have been removed by upwards turbulent and advective transport. However, it does agree with the observed net sedimentation of 1170 mmol m^{-2} $year^{-1}$. There are three possible explanations for the decrease in Si concentrations in the hypolimnion: (i) our estimates of turbulent and advective transport are too low by at least a factor 2, i.e., the lacking 1000 mmol m^{-2} $year^{-1}$ was transported upwards, consumed by the diatoms and added to the gross sedimentation; (ii) the decrease in Si concentrations was strongly overestimated by Shimaraev and Domysheva (2002); or (iii) there is a direct sink of Si from the hypolimnion to the sediment. There is no convincing evidence for any of these three explanations, and we have to leave this question unanswered.

Second, the upward transport of Si from the deep water to the epilimnion, F_{at}^{Si}, of only 630 mmol m^{-2} $year^{-1}$ agrees perfectly with the sum of the dissolution R_{dh}^{Si}=420 mmol m^{-2} $year^{-1}$ plus the sediment source of R_{ds}^{Si}=240 mmol m^{-2} $year^{-1}$ estimated from diffusion plate profiles. But together with an inflow, F_{in}^{Si}, of 312 mmol m^{-2} $year^{-1}$, it cannot support an export rate, S_{exp}^{Si}, of 2700 mmol m^{-2} $year^{-1}$, even if we assume that the observed annual decrease of 1000 mmol m^{-2} $year^{-1}$ was in fact added to the export rate. Moreover, there was a large discrepancy between the Si mass accumulation rate in sediment cores and the Si flux determined from bottom traps. These fluxes suggest that dissolution of Si from the sediment should be in the order of 1000–1500 mmol m^{-2} $year^{-1}$, which is four to six times more than what we estimated from porewater concentration measurements. This indicates that the settling flux of silica during the time of exposition of the sediment traps was rather high and not in line with the long-term sedimentation regime. A more realistic upper limit for the long-term export of biogenic silica can be estimated to $S_{exp}=S_{net}+F_{dif}+R_{dh}$=1830 mmol m^{-2} $year^{-1}$ instead of the 2700 mmol m^{-2} $year^{-1}$. The reason for the high observed export and gross sedimentation rates may be the above-average occurrence of massive blooms of the diatom aulacoseira baikalensis. The so-called "Melosira-events" occur once every 3 to 5 years, and one event just occurred during our 2-year sampling period. These cause a much higher sedimentation of biogenic silica than in years without such blooms. The estimated long-term average for the export production of particulate Si of 1830 mmol m^{-2} $year^{-1}$ increased by 50% due to the diatom blooms. The exceptional diatom bloom was observed only in the South Basin, while we have no clear indication of a similar diatom bloom in the North Basin. The difference to the flux in the North Basin (1400 mmol m^{-2} $year^{-1}$; Fig. 8b) is about 25%, which is in line with the ratio of C and N between South and North Basins. Net sedimentation and dissolution from the sediment both were 35% and 37% smaller than in the South Basin. Upward advective and turbulent transport was 27% smaller. Apart from the bottom sediment sample, the Si_{bio} budget for the North Basin of Lake Baikal looks consistent with all fluxes consequently smaller than in the South Basin.

5. Conclusions

Combinations of four entirely different and independent methods in a multidisciplinary collaboration of physicists, biogeochemists, and sedimentologists revealed a coherent picture of nutrient budgets of Lake Baikal. In spite of the enormous size of the lake, it was possible to present consistent budgets for carbon, nitrogen, phosphorus, and silica for the North and South Basins that agreed reasonably well with estimates given in the Russian literature. Fluxes for the South Basin with its large tributaries and sedimentation regions, mainly the Selenga Delta, could be clearly differentiated from those of the North Basin, which has less nutrients, lower water temperatures, and longer ice coverage. O_2 supply to the sediments was almost entirely provided by turbulent transport through the water column. Hence, advective mixing was not a prerequisite for sufficient O_2 content in the bottom waters. The decrease of hypolimnic Si concentration observed over a time period of 5 years from the monitoring data by Shimaraev and Domysheva could not be verified with our physical transport measurements. Based on our sediment trap data from the South Basin, we observed decomposition in the water column of 30% for C_{org}, 20% for N, and 35% for P. 13% C_{org}, 13% N, and 26% P of the total export from the epilimnion were finally buried in the sediment. Net sedimentation of biogenic silica, however, was 64% (South

Basin) and 54% (North Basin) of the amount exported from the epilimnion. Sediment trap data from the South Basin were affected by a periodically occurring bloom of the diatom *Aulacoseira baicalensis* that increased the Si export from the epilimnion by an estimated 50% over the long-term average. Hence, these data overestimated the Si export from the epilimnion to the sediments and call attention to the importance of long-term monitoring data.

Acknowledgement

We are very grateful to the captain and crew of Vereshagin and the organization by Hedi Oberhänsli. Many thanks to Michael Schurter for indispensable support on all expedition issues, Sandra Windlin for the help and company during the expedition 2003, Ruth Stierli for her careful work in the lab, and Wisi Zwyssig for dealing with the sediments, René Gächter for discussions and suggestions for the manuscript, Burchan for his good humor. Valentina Domysheva provided concentration profiles of silica, nitrate, phosphate, and oxygen. The work of Lorenzo Spadini and an anonymous reviewer who helped to improve this manuscript is gratefully acknowledged. This work was partially financed by BBW grant no. 00454. This work was funded by the EU-project CONTINENT (High-resolution CONTINENTal paleoclimate record in the Lake Baikal: A key-site for Eurasian teleconnections to the North Atlantic Ocean and monsoonal system; EVK2-CT-2000-00057).

Appendix A

Raw data for Table 4: position of the sediment master cores, sedimentation rates, sediment density, water content, porosity, mass accumulation rate, and element content.

Site	Sample	Position		Sed. rate	ρ_{sed}	Porosity	MAR	C	N	Si_{bio}	P
	no.	N	E	[mm year^{-1}]	[g cm^{-3}]	–	[g m^{-2} year^{-1}]	[g kg^{-1}]			
Continent Ridge	Baik01-19C	53 57.236	108 54 804	0.57	2.53	0.953	68	22.2	2.8	321	1.19
Posolskoe Bank	Baik01-29M	52 04.661	105 51.453	1.49	2.53	0.929	266	25.6	2.9	114	0.99
Vidrino Site	Baik01-34C	51 34.122	104 51.271	0.75	2.56	0.925	143	21.1	1.7	254	0.76
South Basin center	Baik01-36A	51 42.468	105 01.324	0.47	2.53	0.925	89	26.2	3.1	341	0.75

Appendix B

Concentrations of NO_3^-, NH_4^+, PO_4, and Si from porewaters sampled with diffusion plates. Flux data "D" in Table 1 were calculated from these profiles.

	Maloe More				Academician Ridge				Posolskoe High				Vydrino Shoulder				Continent Ridge				North Basin			
Date	June 29, 1996				June 29, 1996				July 10, 2001				July 11, 2001				July 8, 2002				July 8, 2002			
Depth	125 m				280 m				160 m				674 m				360 m				792 m			
Pos.	53°19.467–107°25.333				53°36.950–108°17.967				52°04.697–105°50.783				51°36.006–104°54.653				53°57.354–1 08°55.030				54°5.049–109°0.420			
Depth	NO_3^-	NH_4^+	P0$_4$	Si	NO_3^-	NH_4^+	P0$_4$	Si	NO_3^-	NH_4^+	P0$_4$	Si	NO_3^-	NH_4^+	P0$_4$	Si	NO_3^-	NH_4^+	P0$_4$	Si	NO_3^-	NH_4^+	P0$_4$	Si
Cm	[µmol l^{-1}]				[µmol l^{-1}]				[µmol l^{-1}]				[µmol l^{-1}]				[µmol l^{-1}]				[µmol l^{-1}]			
1	4.2	3.0	<0.1	nd	<5	1.2	<0.1	67	10	<5	nd	nd	10	<5	1.1	nd	<5	<0.1	<0.1	57	<5	0.2	<0.1	40
2	nd	nd	0.14	63	<5	nd	<0.1	122	11	<5	0.7	17	8	7	1.1	88	<5	1.32	<0.1	49	<5	0.2	<0.1	53

Appendix B (*continued*)

	Maloe More				Academician Ridge				Posolskoe High				Vydrino Shoulder				Continent Ridge				North Basin			
Date	June 29, 1996				June 29, 1996				July 10, 2001				July 11, 2001				July 8, 2002				July 8, 2002			
Depth	125 m				280 m				160 m				674 m				360 m				792 m			
Pos.	53°19.467–107°25.333				53°36.950–108°17.967				52°04.697–105°50.783				51°36.006–104°54.653				53°57.354–1 08°55.030				54°5.049–109°0.420			
Depth	NO_3^-	NH_4^+	$P0_4$	Si	NO_3^-	NH_4^+	$P0_4$	Si	NO_3^-	NH_4^+	$P0_4$	Si	NO_3^-	NH_4^+	$P0_4$	Si	NO_3^-	NH_4^+	$P0_4$	Si	NO_3^-	NH_4^+	$P0_4$	Si
Cm	[μmol l^{-1}]				[μmol l^{-1}]				[μmol l^{-1}]				[μmol l^{-1}]				[μmol l^{-1}]				[μmol l^{-1}]			
3	<1	5.4	0.14	nd	<5	1.7	<0.1	nd	11	<5	0.6	20	11	<5	0.4	97	<5	<0.1	<0.1	59	<5	0.9	<0.1	55
4	nd	nd	<0.1	148	<5	nd	<0.1	73	10	<5	<0.1	22	11	13	<0.1	92	<5	0.90	<0.1	45	<5	1.7	<0.1	55
5	5.3	2.4	<0.1	nd	<5	1.5	<0.1	nd	10	<5	<0.1	53	9	11	0.4	82	<5	0.48	<0.1	54	<5	2.2	<0.1	67
6	nd	nd	<0.1	53	<5	nd	<0.1	63	11	<5	0.3	136	12	3	0.6	57	<5	<0.1	<0.1	68	11.4	2.1	<0.1	119
7	<1	3.9	<0.1	nd	<5	0.7	<0.1	nd	9	1.0	0.2	262	10	5	0.6	96	<5	<0.1	<0.1	117	<5	1.0	<0.1	135
8	nd	nd	<0.1	128	<5	nd	<0.1	60	<5	3.8	0.5	298	11	<5	<0.1	93	<5	0.20	<0.1	154	8.6	0.9	<0.1	143
9	4.7	4.5	0.14	nd	<5	1.2	<0.1	nd	<5	3.4	1.3	340	9	21	0.2	nd	<5	<0.1	<0.1	170	8.2	1.7	<0.1	191
10	nd	nd	<0.1	53	<5	nd	<0.1	22	<5	5.7	0.6	364	8	<5	0.7	94	<5	<0.1	<0.1	197	<5	2.1	<0.1	260
11	4.2	2.0	<0.1	nd	<5	0.6	<0.1	nd	<5	8.4	0.6	422	9	7	<0.1	162	<5	<0.1	<0.1	219	<5	0.9	<0.1	322
12	nd	nd	0.13	117	<5	nd	<0.1	120	<5	10.2	1.5	453	8	5	0.1	184	<5	0.34	<0.1	214	<5	1.4	<0.1	321
13	3.2	2.4	<0.1	nd	<5	0.7	<0.1	nd	<5	10.5	3.1	462	8	7	1.3	239	<5	<0.1	<0.1	236	<5	1.4	<0.1	406
14	nd	nd	0.14	nd	<5	nd	<0.1	65	<5	13.8	3.7	486	<5	12	1.8	295	<5	0.62	<0.1	281	<5	1.0	<0.1	411
15	<1	5.6	0.12	nd	<5	<0.5	<0.1	nd	<5	20.0	nd	502	<5	10	3.7	355	<5	0.62	2.8	352	<5	1.5	<0.1	410
16	nd	nd	<0.1	68	<5	nd	<0.1	61	<5	21.2	8.8	504	<5	16	2.2	398	<5	0.34	3.2	449	<5	1.9	<0.1	393
17	<1	2.7	<0.1	nd	<5	1.0	0.12	nd	<5	16.1	11	502	<5	11	1.6	422	<5	<0.1	3.5	451	<5	1.0	<0.1	410
18	nd	nd	0.16	nd	<5	nd	<0.1	59	<5	15.3	7.7	nd	<5	17	2.8	442	<5	<0.1	3.7	478	<5	0.9	<0.1	448
19	3.9	4.0	0.10	nd	<5	1.0	<0.1	nd	<5	14.3	11	544	<5	21	1.5	451	<5	1.18	4.0	478	<5	0.9	2.9	459
20	4.7	nd	<0.1	108	<5	nd	<0.1	64	<5	14.5	20	540	<5	11	2.4	450	<5	0.76	4.3	517	<5	2.6	3.6	470
21	<1	<0.5	<0.1	nd	<5	<0.5	<0.1	nd	<5	15.4	nd	557	<5	12	3.1	406	<5	0.76	4.7	498	<5	1.5	3.4	473
22	nd	nd	0.13	nd	<5	nd	<0.1	64	<5	15.2	25	566	<5	25	1.5	419	<5	0.20	4.0	445	<5	1.0	3.5	474
23	<1	10.8	0.12	nd	<5	0.9	<0.1	nd	<5	15.9	nd	572	<5	12	1.9	410	<5	0.34	4.1	527	<5	1.7	5.2	486
24	<1	nd	<0.1	88	<5	nd	<0.1	78	<5	16.0	nd	647	<5	13	1.7	408	<5	1.18	4.6	508	<5	1.7	4.3	492
25	1.1	5.6	<0.1	nd	<5	0.6	0.10	nd	<5	16.8	nd	666	<5	10	1.3	431	<5	2.45	4.0	491	<5	1.8	4.6	474
26	<1	nd	0.10	nd	<5	nd	<0.1	114	<5	17.5	<0.1	626	<5	20	0.7	459	<5	2.59	3.0	504	<5	1.0	5.3	477
27	<1	3.6	<0.1	nd	<5	1.1	<0.1	nd	<5	16.8	nd	706	<5	10	1.5	438	<5	0.90	3.9	498	<5	1.1	3.6	455
28	<1	nd	0.10	248	<5	nd	0.10	30	<5	16.5	nd	656	<5	15	1.7	464	<5	0.34	3.7	510	<5	1.0	4.3	471
29	<1	2.5	<0.1	nd	<5	0.7	0.58	nd	<5	16.0	nd	591	<5	<5	2.6	456	<5	<0.1	3.2	507	<5	0.9	5.9	470
30	1.1	nd	<0.1	214	<5	nd	0.94	70	<5	16.7	nd	nd	<5	18	nd	513	<5	0.20	2.1	491	<5	1.5	4.5	479
31	6.3	8.6	<0.1	nd	<5	0.4	0.89	nd	<5	16.0	nd	nd	<5	21	5.0	506	<5	0.62	<0.1	514	<5	1.8	<0.1	454
32	1.3	nd	<0.1	86	<5	nd	1.04	436	<5	16.7	17	593	<5	16	3.7	487	<5	1.74	<0.1	520	<5	2.8	5.0	464
33	2.5	3.1	6.1	nd	<5	1.2	1.06	nd	<5	16.5	13	587	<5	35	0.7	467	<5	1.18	<0.1	477	<5	3.5	4.1	496
34	1.3	nd	12.8	182	<5	nd	0.93	463	<5	17.1	<0.1	697	<5	13	0.3	444	<5	0.76	<0.1	495	<5	6.6	2.7	509
35	2.5	2.7	40.1	nd	<5	2.8	0.31	nd	<5	18.2	nd	nd	<5	nd	4.4	482	<5	1.74	<0.1	513	<5	4.3	<0.1	499
36	<1	nd	51.5	496	<5	nd	0.16	441	<5	18.5	nd	620	<5	15	3.4	480	<5	1.18	<0.1	519	<5	3.6	<0.1	502
37	2.3	3.9	25.4	nd	<5	2.6	<0.1	nd	<5	17.8	13	606	<5	nd	5.9	522	<5	2.17	<0.1	494	<5	4.1	<0.1	495
38	2.3	nd	17.9	334	<5	nd	<0.1	436	<5	18.3	13	nd	<5	nd	nd	485	<5	2.59	<0.1	466	<5	3.2	<0.1	492
39	2.0	2.8	14.9	nd	<5	2.4	<0.1	nd	<5	18.9	23	nd	<5	12	nd	489	<5	2.17	2.5	475	<5	3.3	<0.1	474
40	1.3	nd	12.8	nd	<5	nd	0.10	413	<5	18.9	28	608	<5	11	9.8	467	<5	2.03	2.5	474	<5	3.7	<0.1	478
41	2.0	1.8	14.9	nd	<5	3.4	<0.1	nd	<5	19.7	nd	620	<5	11	2.6	430	<5	2.03	2.7	495	<5	4.3	<0.1	468
42	2.8	nd	10.3	61	<5	nd	<0.1	63	<5	19.7	nd	nd	<5	nd	4.9	509	<5	nd	<0.1	520	<5	5.9	<0.1	470
43	1.4	1.3	7.4	nd	<5	4.4	<0.1	nd	<5	20.7	nd	nd	<5	13	2.2	464	<5	2.03	2.1	513	<5	3.7	<0.1	465
44	1.3	nd	7.4	363	<5	nd	0.17	407	<5	21.8	nd	662	<5	12	5.2	479	<5	2.31	2.0	532	<5	4.0	<0.1	454
45	1.6	2.3	6.5	nd	<5	4.1	0.44	nd	<5	21.1	nd	699	<5	12	2.0	464	<5	1.89	<0.1	488	<5	4.3	<0.1	456
46	2.0	nd	9.1	369	<5	nd	0.20	466	<5	22.0	nd	nd	<5	12	nd	504	<5	1.46	<0.1	521	<5	5.1	<0.1	10
47	1.6	nd	12.8	392	<5	nd	0.24	nd	<5	21.8	nd	nd	<5	14	nd	490	<5	2.45	<0.1	548	<5	4.3	<0.1	10
48	2.1	3.0	24.2	nd	<5	7.2	<0.1	460	<5	22.9	nd	nd	<5	15	6.6	499	<5	2.87	<0.1	571	<5	7.0	<0.1	432

Appendix C

Concentration data of NO_3^-, NH_4^+, PO_4, and Si from filtered sediment porewaters. Basis for the flux data "F" in Table 1.

	Maloe More				Posolskoe High				Vidrino Shoulder				Continent Ridge				Central Basin			
Date	10 July 2003				12 July 03				13 July 03				8 July 03				7 July 03			
Depth	153 m				148 m				721 m				785 m				1630 m			
Core	Baik03-22B				Baik03-23				Baik03-27				Baik03-15				Baik03-2B			
Pos.	53°19.997–107°26.218				52°4.592–105°50.689				51°36.336–104°54.684				54°4.990–109°0.386				53°11.030–107°47.653			
Depth	NO_3^-	NH_4^+	PO_4	SiO_2	NO_3^-	NH_4^+	PO_4	SiO_2	NO_3^-	NH_4^+	PO_4	SiO_2	NO_3^-	NH_4^+	PO_4	SiO_2	NO_3^-	NH_4^+	PO_4	SiO_2
cm	[μmol l^{-1}]				[μmol l^{-1}]				[μmol l^{-1}]				[μmol l^{-1}]				[μmol l^{-1}]			
>0	15.0	0			15.0	0			15.0	0			15.0	0			15.0	0	0	60
0–0.5	32.5	36.5	1.8	166	21.1	40.6	1.6	181	22.4	43.4	2.6	259	23.4	40.4	5.4	182	21.4	45.7	6.3	217
0.5–1	44.5	48.7	1.9	225	16.0	33.7	2.6	245	20.3	26.0	2.6	335	19.1	21.6	6.3	217	11.2	36.0	9.1	301
1–1.5	31.4	24.5	1.9	264	19.7	36.0	2.6	293	15.8	28.3	2.6	390	26.7	25.2	3.2	254	6.4	57.0	12.8	325
1.5–2	7.6	48.8	2.9	345	20.5	17.8	2.2	329	19.9	31.8	3.2	435	nd	27.0	7.5	272	4.6	32.0	10.0	359
2–2.5	18.5	33.1	2.9	360	12.7	15.7	4.1	371	<2	35.9	3.8	481	26.4	35.8	7.9	286	15.0	72.5	nd	365
2.5–3	11.9	29.1	3.5	419	8.4	13.7	3.2	357	6.4	19.4	18.1	531	34.7	37.8	10.0	303	7.4	63.0	7.5	354
3–3.5	13.4	35.0	3.5	446	11.7	27.1	3.5	382	5.9	44.9	7.5	545	nd	25.9	11.6	315	11.3	61.6	3.8	418
3.5–4	18.8	26.0	1.3	464	10.2	nd	4.7	405	12.2	51.8	5.4	525	29.7	32.1	9.4	331	14.5	82.9	3.8	388
4–4.5	12.7	nd	6.6	486	11.0	34.7	6.0	430	8.5	52.5	5.4	592	nd	29.1	12.2	333	16.0	98.5	3.2	344
4.5–5	14.8	27.8	5.4	458	9.4	26.7	3.8	399	9.1	52.2	11.6	621	35.1	15.5	5.7	347	25.4	93.1	2.9	344
5–6	17.0	nd	5.0	433	4.7	37.2	4.7	539	5.9	42.0	21.6	654	28.1	38.8	20.0	344	15.5	100	3.8	353
6–7	12.7	39.7	5.0	455	6.6	53.0	11.6	579	4.9	42.6	9.1	584	nd	49.4	13.8	348	12.5	95.5	6.0	397
7–8	nd	41.2	21.0	483	4.5	44.3	17.2	614	5.2	48.1	35.9	674	25.0	55.7	8.5	359	18.5	121	4.7	382
8–9	19.5	22.9	68.1	491	5.4	43.4	42.8	657	6.9	47.6	17.2	589	30.8	54.7	5.4	363	14.6	95.8	7.5	374
9–10	18.5	46.7	22.5	534	9.5	51.1	16.0	635	7.1	54.8	13.2	598	28.8	13.1	3.8	366	8.5	66.0	11.9	406

Appendix D. Estimation of turbulent diffusion coefficients K_{400} in Lake Baikal

For the calculation of the vertical turbulent fluxes, an estimate of the turbulent diffusion coefficient at 400-m depth, K_{400}, is needed. The vertical diffusion coefficient for the South Basin was derived based on measurements and turbulent kinetic energy balances by Wüest et al. (2000). For the North Basin, the ice-covered period is about 1 month longer and the average wind speed during the ice-free period is only about 3.2 m s^{-1} compared to 4 m s^{-1} for the South Basin (Shimaraev et al., 1994). The average energy input to the lake surface can be estimated by integrating the energy flux $P=\rho_{Air}C_{10}U_{10}^3$ over the ice-free period. Here, ρ_{Air} is the density of air, C_{10} is the wind drag coefficient (Wüest and Lorke, 2003), and U_{10} the wind speed 10 m above the surface. The calculated energy input for the North Basin is approximately 40% of the input to the South Basin. The turbulent diffusivity can then be estimated with the Osborn relation $K_z=\gamma_{mix}\varepsilon/N^2$ (Osborn, 1980), where γ_{mix} is an empirical constant, ε is the energy dissipation, and N^2 the stability of the water column. We assume that γ_{mix} and the ratio of wind energy input and dissipation are the same in both basins. The stability N^2 at 400-m depth is about 2 10^{-8} s^{-2} in the North Basin and 3 10^{-8} s^{-2} in the South Basin (data not shown). From this, we can conclude that the diffusivity in the North Basin equals about 8 cm^2 s^{-1}. This is at least qualitatively confirmed by the simulations of Peeters et al. (2000) who estimated diffusivities of 4.6 cm^2 s^{-1} for the South Basin and 1.7 cm^2 s^{-1} for the North Basin.

Appendix E

Raw data for Table 4: dry weight is the weight of total sedimented matter after freeze-drying. The particle flux was calculated using dry weight, exposure time, and a sediment trap area of 65 cm^2.

Site	Sample	Date	Date	Exposure	Dry weight	Particle flux	C	N	Si_{bio}	P
	No.	In	Out	d	[mg]	[mg m^{-2} d^{-1}]	[g kg^{-1}]			
South mooring	01-SZ 2	12.Mar.01	5.Jul.02	480	1181.9	378.8	86.1	9.4	632	1.26
	01-SZ 13	12.Mar.01	5.Jul.02	480	1001.7	321.1	68.0	8.0	511	1.38
Neutrino site	01 z-2	8.Mar.01	7.Mar.02	364	813.7	343.9	88.9	8.1	510	2.19
	01 z-13	8.Mar.01	7.Mar.02	364	879.0	371.5	73.3	6.7	500	0.97
North mooring	01-NZ 2	4.Jul.01	5.Jul.02	366	408.1	171.6	129.9	12.3	627	1.27
	01-NZ 8	4.Jul.01	5.Jul.02	366	612.5	257.5	47.9	4.5	692	0.88

References

Appleby, P.G., 2000. Chronostratigraphic techniques in recent sediments. In: Last, W.M., Smol, J.P. (Eds.), Developments in Paleoenvironmental Research.

Back, S., De Batist, M., Strecker, M.R., Vanhauwaert, P., 1999. Quaternary depositional systems in northern Lake Baikal, Siberia. J. Geol. 107 (1), 1–12.

Bender, M.L., Martin, W., Hess, J., Sayles, F., Ball, L., Lambert, C., 1987. A whole-core squeezer for interfacial pore-water sampling. Limnol. Oceanogr. 32, 1214–1225.

Berner, R.A., 1980. Early Diagenesis, A Theoretical Approach. Princeton University Press, Princeton, USA.

Callender, E., Granina, L., 1997. Biogeochemical phosphorus mass balance for Lake Baikal, southeastern Siberia, Russia. Mar. Geol. 139 (1–4), 5–19.

Callender, E., Granina, L., 1997. Geochemical mass balances of major elements in Lake Baikal. Limnol. Oceanogr. 42 (1), 148–155.

Deike, R.G., Granina, L., Callender, E., McGee, J.J., 1997. Formation of ferric iron crusts in quaternary sediments of Lake Baikal, Russia, and implications for paleoclimate. Mar. Geol. 139 (1–4), 21–46.

DEW, 1996. Deutsche Einheitsverfahren zur Wasseruntersuchung (DEW), Weinheim.

Domysheva, V.M., 2001. Spatial distribution patterns and dynamics of oxygen and biogenic elements in the deep water region of Baikal. PhD thesis, University of Irkutsk, Irkutsk.

Falkner, K.K., Measures, C.I., Herbelin, S.E., Edmond, J.M., Weiss, R.F., 1991. The major and minor element geochemistry of Lake Baikal. Limnol. Oceanogr. 36 (3), 413–423.

Granina, L., 1997. The chemical budget of Lake Baikal: a review. Limnol. Oceanogr. 42 (2), 373–378.

Granina, L., Tomza, U., Arimoto, R., Grachev, A., Granin, M., 2000. A study of the chemical budget of Lake Baikal using neutron activation and synchrotron radiation. Nucl. Instrum. Methods Phys. Res., Sect. A, Accel. Spectrom. Detect. Assoc. Equip. 448 (1–2), 419–424.

Granina, L.Z., Müller, B., Wehrli, B., 2004. Origin and dynamics of Fe- and Mn-sedimentary layers in Lake Baikal. Chem. Geol. 205 (1–2), 55–72.

Hakanson, L., Jansson, M., 1983. Principles of Lake Sedimentology. Springer-Verlag, Germany.

Hesslein, R.H., 1976. An in situ sampler for close interval pore water studies. Limnol. Oceanogr. 21, 912–914.

Hohmann, R., Kipfer, R., Peeters, F., Piepke, G., Imboden, D.M., Shimaraev, M.N., 1997. Deep-water renewal in Lake Baikal. Limnol. Oceanogr. 42 (5), 841–855.

Hohmann, R., Hofer, M., Kipfer, R., Peeters, F., Imboden, D.M., Baur, H., Shimaraev, M.N., 1998. Distribution of helium and tritium in Lake Baikal. J. Geophys. Res., Oceans 103 (C6), 12823–12838.

Jahnke, R.A., 1988. A simple, reliable, and inexpensive pore-water sampler. Limnol. Oceanogr. 33, 483–487.

Kelts, K., Briegel, U., Ghilardi, K., Hsü, K., 1986. The limnogeology–ETH coring system. Schweiz. Z. Hydrol. 48, 104–115.

Killworth, P.D., Carmack, E.C., Weiss, R.F., Matear, R., 1996. Modeling deep-water renewal in Lake Baikal. Limnol. Oceanogr. 41 (7), 1521–1538.

Kipfer, R., Hofer, M., Peeters, F., Imboden, D.M., Domysheva, V.M., 2000. Vertical turbulent diffusion and upwelling in Lake Baikal estimated by inverse modeling of transient tracers. J. Geophys. Res., Oceans 105 (C2), 3451–3464.

Kodenev, G.G., Shimaraev, M.N., Shishmarev, A.T., 1998. Determination of the time-scale of the Baikal deep-water renewal with the use of chemical tracers. Geol. Geofiz. 39 (6), 842–850.

Kozhova, O.M., Izmest'eva, L.R., 1998. Lake Baikal. Evolution and Biodiversity. Backhuys Publisher, Leiden, 447 pp.

Li, Y.H., Gregory, S., 1974. Diffusion of ions in seawater and in deep-sea sediments. Geochim. Cosmochim. Acta 38, 703–714.

Mackay, A.W., Battarbee, R.W., Flower, R.J., Granin, N.G., Jewson, D.H., Ryves, D.B., Sturm, M., 2003. Assessing the potential for developing internal diatom-based transfer functions for Lake Baikal. Limnol. Oceanogr. 48 (3), 1183–1192.

Maerki, M., Wehrli, B., Dinkel, C., Müller, B., 2004. The influence of tortuosity on molecular diffusion in freshwater sediments of high porosity. Geochim. Cosmochim. Acta 68 (7), 1519–1528.

Maerki, M., Müller, B., Wehrli, B., submitted for publication. New perspectives to assess mineralization pathways in surface sediments. Limnol. Oceanogr.

Martin, P., Granina, L., Martens, K., Goddeeris, B., 1998. Oxygen concentration profiles in sediments of two ancient lakes: Lake Baikal (Siberia Russia) and Lake Malawi (East Africa). Hydrobiologia 367, 163–174.

Middelburg, J.J., Soetaert, K., Herman, P.M.J., Heip, C.H.R., 1996. Denitrification in marine sediments: a model study. Glob. Biogeochem. Cycles 10 (4), 661–673.

Mortlock, R.A., Froehlich, P.N., 1989. A simple method for the rapid determination of biogenic opal in pelagic marine sediments. Deep-Sea Res. 36 (9), 1415–1426.

Müller, B., Granina, L., Schaller, T., Ulrich, A., Wehrli, B., 2002. P, As, Sb, Mo, and other elements in sedimentary Fe/Mn layers of Lake Baikal. Environ. Sci. Technol. 36 (3), 411–420.

Munk, W.H., 1966. Abyssal recipes. Deep-Sea Res. 13, 707–730.

Osborn, T.R., 1980. Estimates of the local rate of vertical diffusion from dissipation measurements. J. Phys. Oceanogr. 10, 83–89.

Peeters, F., Kipfer, R., Hohmann, R., Hofer, M., Imboden, D.M., Kodenev, G.G., Khozder, T., 1997. Modeling transport rates in Lake Baikal: gas exchange and deep water renewal. Environ. Sci. Technol. 31 (10), 2973–2982.

Peeters, F., Kipfer, R., Hofer, M., Imboden, D.M., Domysheva, V.M., 2000. Vertical turbulent diffusion and upwelling in Lake Baikal estimated by inverse modeling of transient tracers (vol 105, pg 3451, 2000). J. Geophys. Res., Oceans 105 (C6), 14283.

Ravens, T.M., Kocsis, O., Wüest, A., Granin, N., 2000. Small-scale turbulence and vertical mixing in Lake Baikal. Limnol. Oceanogr. 45 (1), 159–173.

Ryves, D.B., Jewson, D.H., Sturm, M., Battarbee, R.W., Flower, R.J., Mackay, A.W., Granin, N.G., 2003. Quantitative and qualitative relationships between planktonic diatom communities and diatom assemblages in sedimenting material and surface sediments in Lake Baikal, Siberia. Limnol. Oceanogr. 48 (4), 1643–1661.

Shimaraev, M.N., Domysheva, V.M., 2002. Dynamics of dissolved silica in Lake Baikal. Dokl. Earth Sci. 387A (9), 1075–1078.

Shimaraev, M.N., Granin, N., 1991. Temperature stratification and the mechanism of convection in Lake Baikal. Dokl. Akad. Nauk 321, 831–835.

Shimaraev, M.N., Verbolov, V.I., Granin, N., Sherstayankin, P.P., 1994. Physical limnology of Lake Baikal: a review. Irkutsk, Okayama, 80 pp.

Tarasova, E.N., Mescheryakova, A.I., 1992. Modern state of hydrochemical regime of Lake Baikal (in Russian). Nauka, Novosibirsk.

Urban, N.R., Dinkel, C., Wehrli, B., 1997. Solute transfer across the sediment surface of a eutrophic lake: 1. Porewater profiles from dialysis samplers. Aquat. Sci. 59 (1), 1–25.

Vologina, E.G., Sturm, M., Vorobyeva, S.S., Granina, L.Z., Toshchakov, S.Y., 2003. Character of sedimentation in Lake Baikal in the Holocene. Russ. Geol. Geophys. 44 (5), 407–421.

Weiss, R.F., Carmack, E.C., Koropalov, V.M., 1991. Deep-water renewal and biological production in Lake Baikal. Nature 349 (6311), 665–669.

Wüest, A., Lorke, A., 2003. Small-scale hydrodynamics in lakes. Annu. Rev. Fluid Mech. 35, 373–412.

Wüest, A., Granin, N., Kocsis, O., Ravens, T.M., Schurter, M., Sturm, M., 2000. Deep Water Renewal in Lake Baikal—matching turbulent kinetic energy and internal cycling. Terra Nostra 9, 60–74.

Wüest, A., Ravens, T.M., Kocsis, O., Schurter, M., Sturm, M., Granin, N., 2005. Cold intrusions in Lake Baikal-direct observational evidence for deep water renewal. Limnol. Oceanogr. 50 (1), 184–196.